

CHAPTER 7

ANALYSIS OF Laterally Loaded Pile Groups

7.1 INTRODUCTION

This chapter describes a procedure for analyzing the response of pile groups to lateral loads. The accuracy of the procedure was evaluated by comparing the computed response of the pile groups at the Kentland Farms load test facility to the results of the load tests discussed in Chapter 6. The analyses were performed using the “group-equivalent pile” method, which was developed during the course of this research. The “group-equivalent pile” (abbreviated GEP) method makes it possible to analyze a pile group using computer programs developed for analyzing single piles, such as *LPILE Plus 3.0* (1997).

The GEP method involves the following elements:

- Step 1. A method for developing p-y curves for single piles in soils with friction, soils with cohesion, and soils with both friction and cohesion.
- Step 2. A method for modeling the resistance of pile groups to lateral loading, including group effects and rotational restraint due to the cap.
- Step 3. A method for computing p-y curves for pile caps in soils with friction, cohesion, or both friction and cohesion.

The development and application of the procedure are described in the following sections.

7.2 SINGLE PILE MODEL

7.2.1 Background

The laboratory tests described in Chapter 5 and the field load tests performed on two HP 10 x 42 piles provide a basis for development of p-y curves for the partly saturated silty and clayey soils (natural soils) at the field test facility. The soil parameters used to develop p-y curves for the natural soils are summarized in Figure 7.1.

The piles were analyzed using the computer program *LPILE Plus 3.0* (1997). This program uses finite difference numerical methods to solve the beam bending equation and nonlinear p-y curves to model the soil. *LPILE Plus 3.0* contains “default” p-y curve formulations that can be used for cohesive soils, cohesionless soils, and silts. These formulations are empirical, and are based on pile load tests performed in Texas by Matlock (1970), Reese et al. (1974), Reese and Welch (1975), and others.

As an alternative to “default” p-y curves, the program user can input p-y curves developed using other formulations, as was done in this study. The following subsection describes the procedure that was used to develop p-y curves for modeling the soil conditions encountered at the test site.

7.2.2 Single Pile p-y Curves

There are a number of formulations available for developing p-y curves. These are often empirically related to values of soil strength and stress-strain characteristics, which can be measured in the field or laboratory. Most of these methods use a cubic parabola to model the relationship between p and y. The general form of the cubic parabola relationship is expressed as follows:

$$p = 0.5 p_{ult} \left[\frac{y}{(A \epsilon_{50} D)} \right]^n \quad \text{Equation 7.1}$$

where p is the soil resistance (force per length units); p_{ult} is the maximum value of p at large deflections (force per length units); y is the lateral deflection of a pile at a particular depth (length units); D is the diameter or width of the pile (length units); ϵ_{50} is the strain required to mobilize 50 % of the soil strength (dimensionless); A is a parameter that controls the magnitude of deflections (dimensionless); and n is an exponent (dimensionless), which equals 0.33 for a cubic parabola.

The cubic parabola formulation was used to calculate p - y curves in this study using the procedure developed by Mokwa et al. (1997) for evaluating the lateral response of piles and drilled shafts in partially saturated soils. This p - y curve formulation was found by Mokwa et al. (1997) to be more accurate than the c - ϕ formulation developed by Reese (1997) for silty soils. Load-deflection curves computed using the Reese (1997) and the Mokwa et al. (1997) p - y formulations are compared to measured load-deflection response curves in Section 7.2.4, for piles embedded in partially saturated natural soils at the Kentland Farms facility.

Brinch Hansen's (1961) ultimate load theory forms the basis of the Mokwa et al. (1997) procedure for developing p - y curves, as described in the following paragraphs.

Evans and Duncan (1982) developed an approach based on Brinch-Hansen's (1961) ultimate load theory to determine values of p_{ult} for soils that have both cohesion and friction (c - ϕ soils). Field load tests performed by Helmers et al. (1997) showed that Brinch-Hansen's theory resulted in values of ultimate load capacity for drilled shafts that agreed well, on the average, with the results of field load tests performed in partially saturated soils at 5 sites in Virginia.

In some cases, Brinch-Hansen's theory underestimated the load capacity, and in other cases, it overestimated the capacity. To improve the reliability of Brinch-Hansen's theory for partly saturated silty and clayey soils, Helmers et al. (1977) recommended that theoretical values of soil resistance using Brinch-Hansen's theory should be reduced by 15 %, so that the actual capacities would not be overestimated for any of the test sites. This can be

accomplished by multiplying the theoretical values by a modification factor M , with M having a value of 0.85.

With this empirical adjustment to improve the reliability of the theory, Brinch-Hansen's (1961) theory can be used to express values of p_{ult} as follows:

$$p_{ult} = (\gamma x K_q + cK_c)MD \quad \text{Equation 7.2}$$

where M is an empirical modification factor = 0.85 (dimensionless); D is the pile width or diameter (length units); γ is the moist unit weight of foundation soil (force per volume units); x is the depth measured from the ground surface (length units); c is the cohesion of the foundation soil (force per area units); K_q is a coefficient for the frictional component of net soil resistance under 3D conditions (dimensionless); and K_c is a coefficient for the cohesive component of net soil resistance under 3D conditions (dimensionless).

The principal advancement made in Brinch-Hansen's (1961) theory was the development of expressions for K_q and K_c . These factors vary with depth below ground surface and depend on the values of the soil friction angle, ϕ . The expressions used to evaluate K_q and K_c are given in Appendix E. It can be seen that these are quite complex. Once programmed in a spreadsheet, however, they can be evaluated easily.

7.2.3 Calculations for p-y Curves

The spreadsheet *PYSHEET* Mokwa et al. (1997) was developed to facilitate p-y curve calculations. *PYSHEET* has been renamed to *PYPILE*, and is included as a worksheet in the workbook named *PYCAP*, which is described in subsequent sections of this chapter. Printed output from *PYPILE* is shown in Figure 7.2. This spreadsheet incorporates Brinch Hansen's expressions for K_c and K_q and includes the modification factor, M , used by Helmers et al. (1997) to improve the reliability of Brinch-Hansen's (1961) theory. The studies described here were performed with $M = 0.85$, but the value of M can be varied in the spreadsheet if desired.

The spreadsheet can be used to calculate p-y curves for piles or drilled shafts of any size in c- ϕ soils, and the soil properties and the pile or shaft diameter can be varied with depth.

The parameter A is an empirical adjustment coefficient that can be determined by performing back analyses of field lateral load tests, or by estimating its value based on data for similar soils. The value of A can range from 0.35 to 2.65 (Evans 1982). Reese et al.'s (1974) p-y formulation for sand is based on other equations, but provides results that are comparable to the cubic parabola formulation using an A value of 2.5. Using the results from load tests performed at five sites around the state of Virginia, Mokwa et al. (1997) back-calculated a range of A values that varied from 0.72 to 2.65. An A value equal to 2.5 was found to provide the best overall match between calculated and measured load-deflection curves for the foundations tested at the Kentland Farms site. This value was used for all the p-y curve computations described in this chapter.

7.2.4 Comparison of Measured and Calculated Deflections of Single Piles

Load-deflection response curves for the north and south piles were calculated using p-y curves computed using the computer spreadsheet *PYPILE*. Soil parameters used in the calculations were obtained from laboratory tests, which are summarized in Figure 5.8. Values for p-y curves were calculated using the pile model shown in Figure 7.1, and are plotted in Figure 7.3(a). The p-y values were input into *LPILE Plus 3.0* to calculate the response of single piles to lateral loading. Response curves generated by *LPILE Plus 3.0* include load versus deflection, load versus moment, and load versus shear distributions along the pile length.

All of the load-deflection curves shown in this chapter are referenced to pile deflections at the ground surface, as shown in Figure 7.4. The response curves shown in the following comparisons were obtained from the tests using the strut connection shown in Figure 6.6. As discussed in Chapter 6, tests were also performed using a clevis pin connection (Figure 6.5). Although the intent was to form a freely rotating connection with the clevis pin, the pinned connection was not effective. The spacing of the clevis tongue and yoke plates

were so close that they bound when loaded. Although modifications were attempted, an effective pin connection was not achieved. For this reason, there was no significant difference in the test results between the rigid strut and the clevis pin connection.

Measured load-deflection and load-rotation response curves for the south pile are shown in Figure 7.5. The north pile measured load-deflection curve is not shown because it was almost identical to that of the south pile (see Figure 6.8). Calculated load-deflection curves are compared to the measured response curve for the south pile in Figure 7.6. The calculated response curves were obtained using p-y curves from *PYPILE* with the Mokwa et al. (1997) formulation. As shown in Figure 7.6(a), the pile-head restraining condition falls between a pure fixed-head (zero slope) and a pure free-head (zero moment) condition. A third response curve was calculated for a rotationally restrained pile-head by back-calculating the rotational restraint $k_{m\theta}$. As shown in Figure 7.6(b), a $k_{m\theta}$ value of 5.5×10^7 in-lb/rad was found to provide the best match between calculated and observed load-deflection responses. This illustrates the importance of accurately quantifying the pile-head rotational stiffness.

The *LPILE Plus 3.0* analyses were repeated using the “default” silt p-y curve formulation that was developed by Reese (1997) for soils that possess both cohesion and friction. This p-y curve formulation is not a true c- ϕ method. It involves a combination of two separate formulations, one for sand (the contribution of ϕ) the other for clay (the contribution of c). The p-y curves are generated by adding the ϕ resistance determined using the empirically based p-y formulation for sand with the c resistance determined using the empirically based method for soft clay below the water table. According to the *LPILE Plus 3.0* users manual, the procedure has not been validated by experimental data.

The soil parameters shown in Figure 7.1 were used to develop p-y curves in *LPILE Plus 3.0* using the default silt option. As shown in Figure 7.7(a), neither the fixed-head or free-head boundary conditions provide very accurate predictions of the load-deflection behavior. A third response curve was calculated for a rotationally restrained pile-head by back-calculating the rotational restraint $k_{m\theta}$. As shown in Figure 7.7(b), a $k_{m\theta}$ value of $4.0 \times$

10^8 in-lb/rad was found to provide the best match between calculated and observed load-deflection responses. This value is approximately 7 times as large as the value back calculated using p-y curves from *PYPILE* ($k_{m\theta} = 5.5 \times 10^7$ in-lb/rad). A load-deflection curve calculated using $k_{m\theta} = 5.5 \times 10^7$ in-lb/rad together with the *LPILE Plus 3.0* default p-y silt option is also shown in Figure 7.7(b).

7.2.5 Single Pile Rotational Restraint

The restraining moment (or the moment that resists pile rotation) can be calculated using the estimated value of $k_{m\theta}$ and the measured rotation at the pile head, which was 0.029 radians at a load of about 75 kips. Based on the back-calculated value of $k_{m\theta}$ determined using the p-y curves generated with PYSHEET, the restraining moment is calculated as follows:

$$k_{m\theta} = \frac{M}{\theta} = 4580 \frac{ft - kips}{rad} \quad \text{Equation 7.3a}$$

$$M = \left(4580 \frac{ft - kips}{rad} \right) (0.0294 \text{ rad}) = 135 \text{ ft} - kips \quad \text{Equation 7.3b}$$

A conceptual diagram of the loading connections at the pile-head is shown in Figure 7.8(a). As can be seen in Figure 6.6, the strut was rigidly bolted to the pile. However, the load cell was not rigidly attached to the strut, but was held in place using four 3/4-inch-diameter threaded rods. The threaded rods did not prevent the load cell from rotating. Consequently, as the pile deflected and tilted in the direction of load, the load cell rotated, causing a vertical force to develop at the end of the strut. This vertical force, V , created a moment at the pile of magnitude $V \times w$. Where w is the moment arm, as shown in the free body diagram, Figure 7.8(b).

Using the calculated value of M , and assuming $V = P$, the value of w can be calculated as follows:

$$w = \frac{M}{V} = \frac{135 \text{ ft-kips}}{75 \text{ kips}} = 1.8 \text{ ft} \quad \text{Equation 7.3c}$$

The load transfer mechanism between the load cell, threaded rods, and strut is difficult to quantify. Based on the diagrams shown in Figure 7.8, the calculated value of $w = 1.8$ feet appears reasonable. This indicates that the back-calculated value of rotational restraint, $k_{m\theta} = 5.5 \times 10^7$ in-lb/rad (based on *PYPILE* p-y values) provides a relatively accurate approximation of the boundary conditions at the pile head.

The same series of calculations were repeated using the results obtained from Reese's (1997) default silt p-y curves. A moment arm, w , of 13 feet was calculated from the best fit value of $k_{m\theta} = 4.0 \times 10^8$ in-lb/rad (see Figure 7.7b). A 13-foot-log moment arm does not agree well with the actual load test configuration, and leads to a resisting moment that is larger than physically possible. The *LPILE Plus 3.0* analysis was repeated using Reese's default silt p-y curves with a more reasonable value of rotational restraint of $k = 5.5 \times 10^7$ in-lb/rad. The resulting load-deflection curve shown in Figure 7.7(b) over-predicts the measured deflections by about 150 % at a load of 75 kips.

The measured rotation or slope at the pile head provides an alternate approach for evaluating the accuracy of the two different p-y formulations. The pile-head slope was measured during the load tests using the telltale shown in Figure 3.8. The measured load versus rotation results are shown in Figure 7.5(b). The best fit value of $k_{m\theta}$ was determined for the two different p-y formulations using the same approach that was used for matching the measured load-deflection curves. The results for the Mokwa et al. (1997) *PYPILE* p-y curves are shown in Figure 7.9(a) and the results for the Reese (1997) *LPILE Plus 3.0* default p-y curves are shown in Figure 7.9(b). The values of $k_{m\theta}$ determined by matching measured deflections and measured slopes are shown below for both p-y formulations.

| p-y curve formulation | $k_{m\theta}$ best match for deflection (in-lb/rad) | $k_{m\theta}$ best match for slope (in-lb/rad) | ratio of $k_{m\theta}$(deflection) to $k_{m\theta}$(slope) |
|---|---|--|---|
| <i>PYPILE</i> Mokwa et al. (1997) | 5.5×10^7 | 4.0×10^7 | 1.37 |
| <i>LPILE Plus 3.0</i> default Reese (1997) | 4.0×10^8 | 1.1×10^8 | 3.64 |

There is some discrepancy between the $k_{m\theta}$ values determined using measured deflection as the fitting criteria and the $k_{m\theta}$ values determined using measured slope as the matching criteria. This discrepancy can be expressed as a ratio of $k_{m\theta}$ (deflection match) to $k_{m\theta}$ (slope match). In principle, the p-y curves will provide a precise representation of the soil conditions when the ratio between $k_{m\theta}$ (deflection match) to $k_{m\theta}$ (slope match) equals 1.0. Based on the ratios shown above, neither of the p-y formulations provide an exact replication of the experimental data. There was a 37 % difference between the best-match $k_{m\theta}$ values determined using the Mokwa et al. (1997) *PYPILE* p-y curves. As shown in Figure 7.10(a), a 37 % difference between $k_{m\theta}$ (slope match) and $k_{m\theta}$ (deflection match) leads to a relatively insignificant difference between calculated load-deflection response curves. However, as shown in Figure 7.10(b) for the *LPILE Plus 3.0* default p-y curves, a 260 % difference between $k_{m\theta}$ (slope match) and $k_{m\theta}$ (deflection match) results in a substantial difference between the calculated load-deflection response curves.

Based on the analyses and load test results described in the preceding paragraphs, it can be seen that Reese's (1997) default silt p-y curves result in a poor match with the response curves for the test piles at the Kentland Farms site. The p-y values generated using *PYPILE* provide more accurate load-deflection results for the partially saturated c- ϕ soils at the test site. *PYPILE* was therefore used for creating pile p-y curves for the remainder of the analyses in this report.

7.3 PILE GROUP MODEL

7.3.1 Background

The single pile model developed in Section 7.2 forms a part of the pile group model. The computer program *LPILE Plus 3.0* (1997) was used to analyze the pile groups at the test facility using the approach outlined below:

1. The piles in a four-pile group were modeled as a single pile with four times the moment of inertia of the actual pile, giving four times the flexural resistance of a single pile.
2. The “p” values for each pile were adjusted to account for group effects using the reduction factors shown in Figure 2.15.
3. The adjusted “p” values were summed to develop the combined “p” values for the group of piles.
4. The pile-head boundary condition of the “group-equivalent pile” was determined by estimating the rotational restraint provided by the pile cap.
5. The model created in steps 1 through 4 (the “group-equivalent pile” model) was analyzed using *LPILE Plus 3.0*, and the results were compared to the results of the load tests on the pile groups.

Details of these steps are described in the following sections.

7.3.2 Group Pile p-y Curves

The group-equivalent pile p-y curves were developed using the conditions and properties shown in Figure 7.1. The analytical approach for pile groups was similar to the single pile approach, except the single pile p-values were adjusted to account for the number of piles, and to account for reduced efficiencies caused by pile-soil-pile interactions. In other words:

$$p = \sum_{i=1}^N p_i f_{mi} \quad \text{Equation 7.4a}$$

where p_i is the p-value for the single pile, f_{mi} is the p-multiplier determined from Figure 2.15, and N is the number of piles in the group.

For the 4-pile groups at the Kentland Farms facility, with piles spaced equally at $4D$, the p values equal:

$$p = (p \text{ single pile}) \times 3.2 \quad \text{Equation 7.4b}$$

The p-y curves calculated using this method are shown in Figure 7.3(b). The *EXCEL* spreadsheet *PYPILE* was used to create p-y curves for the NE, NW, and SE pile groups.

7.3.3 Pile-Head Rotations

Although piles in a group are restrained against rotation by a pile cap, the piles will experience a small amount of rotation during lateral loading. Rotation at the pile-head is caused primarily by: 1) deformation and possibly cracking of concrete at the pile connection to the cap, and 2) rotation of the cap and the pile group caused by vertical movement of the piles.

Flexural cracking of the concrete, in the caps at Kentland Farms, was minimized by using reinforcement in both the top and bottom faces of the cap and by providing a minimum of 5 inches of cover around the piles. Thus, for the pile groups tested in this study, pile-head

rotation caused by deformation or cracking of the concrete was negligible in comparison to the rotational effects associated with vertical movement of the piles.

Rotation of the cap caused by vertical movement of the piles can be significant, depending on the vertical capacities of the piles. During lateral loading, the front of the cap tends to move downward and the back of the cap tends to move upward. The amount of rotation depends primarily on the upward movement of the trailing piles, and is a function of the skin friction that is developed on the piles.

The pile group rotational stiffness concept is shown in Figure 7.11. The magnitude of vertical displacement, Δ_t , is controlled by a number of factors, including skin friction or side resistance, Q_s , end resistance, Q_p , elastic shortening or lengthening of the piles, frictional resistance at the ends of the cap, and rotational resistance developed as the leading edge of the cap “toes” into the soil. Based on the load tests performed during this study, it appears that the largest contribution to restraint is that due to the frictional resistance of the piles.

The movement required to mobilize skin friction is considerably smaller than the movement required to mobilize end resistance, and is relatively independent of the pile size and soil type (Kulhawy 1984). There is no consensus in the literature regarding the amount of movement that is required to mobilize skin friction fully. However, a range from 0.1 to 0.3 inches is usually considered to be reasonable (Davisson 1975, Gardner 1975, and Kulhawy 1984). Values at the high end of this range are most likely associated with bored piles or drilled shafts, while values at the low end of the range are more representative of driven piles. For the purpose of back calculating θ_{ult} , the value of Δ_{ult} was assumed equal to 0.1 inches for the piles in this study.

7.3.4 Pile-Head Rotational Stiffness Calculations

The value of $k_{m\theta}$ is defined as:

$$k_{m\theta} = \frac{M}{\theta} \quad \text{Equation 7.5}$$

where M is the restraining moment that resists rotation, and θ is the angular rotation of the pile head. The value of $k_{m\theta}$ approaches infinity for a pure fixed-head condition (zero slope), and $k_{m\theta}$ is 0 for a pure free-head condition (zero restraining moment, M).

Angular rotation of the pile head is assumed here to be equal to the rotation of the pile cap, which is a function of vertical pile movement. The amount of angular rotation can be determined from geometry as:

$$\theta = \tan^{-1} \frac{2\Delta_t}{S} \quad \text{Equation 7.6}$$

where S is the spacing between the leading and trailing rows of piles.

The ultimate value of bending moment that can be counted on to resist cap rotation, M_{ult} , is a function of the side resistance force from each pile, Q_{si} , and the moment arm, X_i , as follows:

$$M_{ult} = \sum_{i=1}^N Q_{si} X_i \quad \text{Equation 7.7}$$

where N is the number of piles in the group, and X_i is the moment arm, as shown in Figure 7.12(a).

There are a number of recognized methods for estimating Q_{si} , including rational approaches such as the α -method (Tomlinson 1987), β -method (Esrig and Kirby 1979) and the λ -method (Vijayvergiya and Focht 1972). The computer program *SPILE* (1993), available from the FHWA, is useful for estimating pile skin resistance. *SPILE* uses the α -method for performing total stress analyses of cohesive soils and the Nordlund (1963) method for performing effective stress analyses of noncohesive soils. In situ approaches are also available such as the SPT method developed by Meyerhof (1976) or the CPT method by Nottingham and Schmertmann (1975).

Estimates of skin resistance for the piles in this study were made using the α -method (Tomlinson 1987), in which pile skin resistance, Q_s , is given by:

$$Q_s = \alpha S_u A_s \quad \text{Equation 7.8}$$

where α is an adhesion factor that modifies the undrained shear strength, S_u , and A_s is the surface area of the pile shaft or perimeter area. α values depend on the magnitude of S_u , the pile length and diameter, and the type of soil above the cohesive bearing stratum. Because the natural soil at the site is partially saturated, its shear strength consists of both cohesive (c) and frictional (ϕ) components, as described in Chapter 5. An equivalent S_u value was estimated for this c - ϕ soil using the following expression:

$$S_u = c + \sigma_h \tan \phi \quad \text{Equation 7.9}$$

where σ_h is the horizontal stress at the depth of interest. Because the natural soil is overconsolidated and may contain residual horizontal stresses caused by pile driving, it was assumed that σ_h was equal to the vertical stress, σ_v .

Although the soils were relatively homogeneous at the Kentland Farms site, Q_{si} values varied between the three pile groups because of differences in the length of the piles in each group. Pile lengths used in the skin friction analyses were based on the distance from the bottom of the pile cap to the pile tip. There was a 9 inch difference in length between the NE and NW pile groups because the NE 36-inch-deep cap extended 9 inches deeper than the NW 18-inch-deep cap. The piles in the SE group were only driven 10 feet. Because the SE cap was 36 inches deep, the piles extended only 7 feet below the bottom of the cap. Calculated values of Q_{si} for the piles in the three test groups are summarized below.

| <u>Foundation</u> | <u>Pile Length (ft)</u> | <u>Q_{si} per pile (kips)</u> | <u>Avg. S_u (ksf)</u> | <u>Avg. α</u> |
|-------------------|-------------------------|--|------------------------------------|---------------------------------|
| NE group | 16.5 | 78 | 1.50 | 0.98 |
| NW group | 17.25 | 82 | 1.50 | 0.98 |
| SE group | 7 | 30 | 1.32 | 1.0 |

The average values of S_u and α are based on weighted averages with respect to pile length. Skin resistance values (Q_{si}) shown above were used with Equation 7.7 to estimate the limiting value of the restraining moment, M_{ult} . As shown in Figure 7.12(b), the relationship between M and θ is expected to be nonlinear up to M_{ult} . The slope of a line drawn through any point along the M - θ distribution defines the value of $k_{m\theta}$. As shown in Figure 7.13(a), it was assumed the initial nonlinear portion of the M - θ curve could be represented by a cubic parabola. The actual shape of the curve is unknown, but a cubic parabola provides a reasonable approximation.

The relationship between M and θ was simplified for the analyses by approximating the curve by a straight line, as shown in Figure 7.13(a). The corresponding value of $k_{m\theta}$ (the slope of this line) can be computed as follows:

The cubic parabola shown in Figure 7.13(a) can be represented as;

$$M = M_{ult} \left(\frac{\theta}{\theta_{ult}} \right)^{0.33} \quad \text{Equation 7.10a}$$

rearranging terms;

$$\frac{M}{M_{ult}} = \left(\frac{\theta}{\theta_{ult}} \right)^{0.33} \quad \text{Equation 7.10b}$$

when $\frac{\theta}{\theta_{ult}} = 0.5$

$$\frac{M}{M_{ult}} = (0.5)^{0.33} = 0.79 \quad \text{Equation 7.10c}$$

thus, $M = 0.79M_{ult}$ for $\theta = 0.5\theta_{ult}$

and, consequently,

$$k_{m\theta} = \frac{M}{\theta} = \frac{0.79M_{ult}}{0.5\theta_{ult}} = 1.6 \frac{M_{ult}}{\theta_{ult}} \quad \text{Equation 7.10d}$$

For the purpose of these analyses, it was assumed that the rotational restraint, $k_{m\theta}$, is constant up to the value of M_{ult} , as shown in Figure 7.13(b).

Using the relationships developed above, $k_{m\theta}$ can be determined as follows:

$$k_{m\theta} = 1.6 \frac{M_{ult}}{\theta_{ult}} = 1.6 \frac{\sum_{i=1}^N Q_{si} X_i}{\tan^{-1}\left(\frac{2\Delta_t}{S}\right)} \quad \text{Equation 7.11}$$

The value of $k_{m\theta}$ can be estimated using the iterative process described below:

Step 1. The rotational restraint calculated from Equation 7.11 is used as the initial pile head boundary condition.

Step 2. The calculated value of moment at the pile-head (M_{pile}), obtained from the *LPILE Plus 3.0* analysis, is compared to the value of M_{ult} calculated using Equation 7.6.

- If $M_{piles} > M_{ult}$, the analysis is repeated using a smaller value of $k_{m\theta}$. This condition is represented by the square in Figure 7.13(b).
- If $M_{piles} \leq M_{ult}$, the solution is acceptable. This condition is represented by the solid circles in Figure 7.13(b).

Using the approach described in this section, the following values of M_{ult} and $k_{m\theta}$ were calculated for the NE, NW, and SE pile groups.

| <u>Foundation</u> | <u>M_{ult} (in-lb)</u> | <u>k_{mθ} (in-lb/rad)</u> |
|-------------------|--------------------------------|-----------------------------------|
| NE group | 6.29 x 10 ⁶ | 2.01 x 10 ⁹ |
| NW group | 6.54 x 10 ⁶ | 2.09 x 10 ⁹ |
| SE group | 2.44 x 10 ⁶ | 7.82 x 10 ⁸ |

7.3.5 Comparison of Measured and Calculated Pile Group Deflections with No Cap Resistance

Load-deflection curves for the NE, NW, and SE pile groups at the Kentland Farms facility were calculated using *LPILE Plus 3.0* and the procedure described in this chapter, with the Mokwa et al. (1997) p-y curves. Calculated results were compared to the measured load-deflection curves for the pile groups. The first comparisons did not include cap resistance. The calculated results were compared to the load tests performed after soil was removed from the sides and the front of the pile caps.

NE pile group. The piles in the NE group extended 16.5 feet below the cap, which was 3 feet deep. p-y values for the “group-equivalent pile” for this group were computed using *PYPILE*. Calculated load-deflection curves for assumed fixed-head and free-head boundary conditions are shown in Figure 7.14(a). Neither of these conditions provides a reasonable estimate of the measured behavior. At a load of 135 kips, the fixed-head case under-predicts the deflection by 67 %, while the free-head case over-predicts the deflection by over 400 %.

The results obtained using a rotationally restrained pile-head boundary condition are in better agreement with the measured deflections, as shown in Figure 7.14(b). The rotational restraint, $k_{m\theta} = 2.01 \times 10^9$ in-lb/rad, was estimated using the approach described in the previous section. In this case, at a load of 135 kips the calculated deflection was only 17 % greater than the measured deflection, a difference of only 0.04 inches.

NW pile group. The piles in the NW group extended 17.25 feet below the cap, which was 1.5 feet deep. *p-y* values for the equivalent NW-group-pile were computed using *PYPILE*. Calculated load-deflection curves for assumed fixed-head and free-head boundary conditions are shown in Figure 7.15(a). Neither of these conditions provides a reasonable estimate of the measured behavior. At a load of 135 kips, the fixed-head case under-predicts the deflection by 56 %, while the free-head case over-predicts the deflection by over 200 %.

The results obtained using a rotationally restrained pile-head boundary condition are considerably more accurate, as shown in Figure 7.15(b). The rotational restraint, $k_{m\theta} = 2.09 \times 10^9$ in-lb/rad, was estimated using the approach described in the previous section. In this case, at a load of 135 kips the calculated deflection was only 13 % less than the measured deflection, a difference of only 0.03 inches.

SE pile group. The piles in the SE group extended 7 feet below the cap, which was 3 feet deep. *p-y* values for the SE group-pile were computed using *PYPILE*. Calculated load-deflection curves for assumed fixed-head and free-head boundary conditions are shown in Figure 7.16(a). Neither of these conditions provides a reasonable estimate of the measured behavior. At a load of 90 kips, the fixed-head case under-predicts the deflection by 53 %, while the free-head case was extremely over-conservative, predicting failure at a load of about 40 kips.

The results obtained using a rotationally restrained pile-head boundary condition are shown in Figure 7.16(b). The rotational restraint, $k_{m\theta} = 7.82 \times 10^8$ in-lb/rad, was estimated using the approach described in the previous section. At a load of 135 kips, the calculated deflection was approximately 100 % greater than the measured deflection, a difference of about 0.34 inches. Although not as accurate as in the cases of the NE and NW pile groups, the calculations are more accurate than assuming fixed-head or free-head conditions, and provide a conservative approximation that would be reasonable for use in design.

In summary, the method that was developed for estimating the lateral capacity of pile groups provided results that were in reasonable agreement with full-scale lateral load tests at

the NE and NW pile groups. The largest difference between calculated and measured load-deflection results occurred for the SE group, which had the shortest piles. The author believes that as the pile lengths decrease, other factors begin to have greater effects on the rotational restraint of the pile head. Piles as short as 7 feet would not typically be used unless they were driven to refusal in a firm bearing strata. The short piles beneath the SE cap were not driven to refusal, and have very small axial capacities. The rotations of the cap will be controlled by the uplift capacity of the trailing piles. Consequently, the SE cap will experience larger rotations because of the small amount of skin resistance that can be developed by its shorter piles. It seems likely that the accuracy of the procedure could be improved by varying the value of $k_{m\theta}$ to represent a nonlinear variation of M with θ . However, this would complicate the procedure to such an extent that it would be too time-consuming for use in routine practice.

7.4 PILE CAP MODEL

7.4.1 Background

Load tests conducted during this study indicate that pile caps provide considerable resistance to lateral loads. This section describes the procedures that were developed for estimating cap resistance using an approach that can be readily coupled with the procedures for analyzing single piles and groups of piles. The approach provides a method for computing the cap resistance derived from passive earth pressures, and models the variation of this resistance with cap deflection using hyperbolic p - y curves. As described in the following paragraphs, the hyperbolic p - y curves are defined by the ultimate passive force and the initial elastic stiffness of the embedded pile cap.

7.4.2 Passive Earth Pressure Resistance

The log spiral earth pressure theory was used to estimate the passive pressure developed on pile caps. The log spiral failure surface consists of two zones: 1) the Prandtl zone, which is bounded by a logarithmic spiral, and 2) the Rankine zone, which is bounded by a plane, as shown in Figure 7.17(a). The shape of the log spiral surface is shown in Figure

7.17(b). For large values of the wall friction angle, δ , the theory is more accurate than Rankine or Coulomb's earth pressure theories, which apply only to simple states of stress, or use plane surfaces to approximate the failure surface. The log spiral, Rankine, and Coulomb theories provide identical results when the wall friction angle, δ , is zero. However, K_p values estimated using Coulomb's theory are non-conservative, and can be very inaccurate for δ values greater than about 0.4ϕ . On the other hand, Rankine's theory does not account for wall friction, and, consequently, may greatly underestimate passive earth pressures, especially at larger values of δ .

The wall friction angle at the front face of a pile cap will be large because of the restraint against vertical movement of the cap that is provided by the piles. For this reason, the log spiral earth pressure theory is the most appropriate theory for estimating the ultimate passive pressure developed by pile caps.

Log spiral earth pressure forces can be determined using a trial and error graphical process based on the principle that a force vector acting on the log spiral failure surface makes an angle of ϕ with the tangent to the spiral, and the lines of action of the force vectors pass through the center of the spiral, as shown in Figure 7.18. This approach can provide accurate results for any magnitude of wall friction, and can also account for cohesion in c - ϕ soils. However, the graphical procedure is time-consuming, and is not adaptable to computer calculations. Caquot and Kerisel (1948) developed tables that can be used for estimating the earth pressure coefficient, K_p , based on the log spiral theory. These tables are available in many foundation engineering text books and manuals. The disadvantages of the tables are that they cannot be used in computer programs, and that they do not account for cohesion.

An *EXCEL* spreadsheet was developed by Dr. J.M. Duncan and the author to calculate passive earth pressures using the log spiral earth pressure theory, and was extended significantly during the course of this study. In its present form, the program accounts for friction, cohesion, and surcharge components of passive pressures, and any magnitude of wall friction. The program is coded in an *EXCEL* workbook named *PYCAP*, which was developed

for calculating p-y curves for embedded pile caps. The workbook *PYCAP* contains a number of different worksheets. The log spiral calculations are performed in the worksheet named *Log Spiral*. Details of the log spiral earth pressure theory, and the worksheet *Log Spiral*, are provided in Appendix F.

The magnitude of the interface wall friction angle and the effects of wall friction on passive earth pressures have been the focus of numerous studies including the classic retaining wall studies by Terzaghi (1932, 1934a, and 1934b), the interface tests performed on dense sands and concrete by Potyondy (1961), and the finite element studies by Clough and Duncan (1971). These studies and others indicate that wall friction is not an absolute value but depends on the amount of wall movement as well as on the soil properties and the properties of the soil/wall interface. In practice, average values of wall friction are often used based on engineering judgement and experience. δ values used in practice most often fall within the range of about 0.4ϕ to 0.8ϕ . Recommended values of δ for use in design are summarized in Table 7.1 for various types of soils and interface materials.

The passive earth pressure force, E_p , can be expressed in terms of its three primary components: 1) soil weight and friction, $P_{p\phi}$, 2) soil cohesion, P_{pc} , and 3) surcharge, P_{pq} . E_p , which is in units of force per unit length, can be expressed as:

$$E_p = (P_{p\phi} + P_{pc} + P_{pq}) \quad \text{Equation 7.12a}$$

or, in terms of earth pressure coefficients:

$$E_p = \frac{1}{2} \gamma H^2 K_{p\phi} + 2cHK_{pc} + qHK_{pq} \quad \text{Equation 7.12b}$$

where the earth pressure coefficient for friction and soil weight is defined as:

$$K_{p\phi} = \frac{2P_{p\phi}}{\gamma H^2} \quad \text{Equation 7.13a}$$

the earth pressure coefficient for cohesion is defined as:

$$K_{pc} = \frac{P_{pc}}{2cH} \quad \text{Equation 7.13b}$$

and the earth pressure coefficient for surcharge is defined as:

$$K_{pq} = \frac{P_{pq}}{qH} \quad \text{Equation 7.13c}$$

The $K_{p\phi}$ value determined using the log spiral method approaches the Rankine value of K_p as δ approaches zero. For this reason, and because numerical difficulties occasionally occur when δ is less than 2 degrees, *PYCAP* automatically defaults to the Rankine value of K_p when δ is less than 2 degrees. In this case, the ultimate passive force, E_p , is expressed in terms of force per unit length as:

$$E_p = \frac{1}{2} \gamma H^2 K_p + 2cH \sqrt{K_p} + qH K_p \quad \text{Equation 7.14}$$

where K_p is determined from Rankine theory as:

$$K_p = \tan^2 \left(45 + \frac{\phi}{2} \right) \quad \text{Equation 7.15}$$

The value of E_p calculated using either of the approaches described above is modified by applying a factor to account for three-dimensional effects. This factor, called R , is discussed in Section 7.4.3. The 3-D passive earth pressure force, P_{ult} is thus determined from E_p as follows:

$$P_{ult} = E_p R b \quad \text{Equation 7.16}$$

where P_{ult} is the ultimate passive earth pressure force (force units), R is a correction factor for 3-D effects (dimensionless), and b is the width of footing or length of wall (length units).

When $\phi = 0$, *PYCAP* defaults to a different method for calculating passive earth pressure, which is called the $\phi = 0$ sliding wedge method. The method closely follows the approach developed by Reese (1997) for modeling the failure zone in front of a laterally loaded pile. This approach assumes that the ground surface rises and translates in the direction of load. The failure wedge is represented as a plane surface, as shown in Figure 7.19. The semi-empirical equation used to calculate the passive earth pressure force is:

$$P_{ult} = \frac{cbH}{2} \left(4 + \frac{\gamma H}{c} + \frac{0.25H}{b} + 2\alpha \right) \quad \text{Equation 7.17}$$

where α is a factor that accounts for adhesion between the cohesive soil and the wall. Typical values of α are shown in Table 7.2. Conservative values of α should be used if there is a possibility that adhesion between the soil and wall could be lost or destroyed by water, frost action or remolding during cyclic loading.

The development of Equation 7.17 is described in Appendix G. This equation is based on full-scale test results, thus it implicitly includes three-dimensional and shape effects and, consequently, additional modifications using the 3-D shape factor are not necessary.

Appendices F and G describe the equations and approaches used to calculate the ultimate passive earth pressure force. As discussed in Section 7.4.3, for values of $\phi > 0$, this force is modified in *PYCAP* for three-dimensional effects using factors developed by Ovesen (1964) from experiments on embedded anchor blocks. This modified ultimate earth pressure force is incorporated into a hyperbolic formulation to develop pile cap p-y values for lateral load analyses. The entire process, including the generation of pile cap p-y values, is automated in the program *PYCAP*. The next section describes the procedure used to modify two-dimensional plane strain passive earth pressures to model three-dimensional behavior.

7.4.3 Three-Dimensional Effects

Load tests were performed on the bulkhead at the field test facility to study the relationship between passive pressures and deflections. Because the bulkhead had no piles, its

resistance to lateral load was provided almost entirely by passive pressure. Frictional resistance on its sides and base was negligibly small. Load tests were conducted to failure for the bulkhead embedded in natural ground, and after backfilling in front of it with crusher run gravel. Measured load versus deflection results are shown in Figure 7.20.

Various methods were examined for calculating the ultimate resistance of the bulkhead, using soil shear strength parameters that were developed from the laboratory tests. These methods included the classical Rankine, Coulomb, and log spiral earth pressure theories; the sliding wedge formulation described by Reese and Sullivan (1980); Brinch Hansen's (1961) ultimate load theory; and Ovesen's (1964) procedure to correct for three-dimensional effects. The most accurate results for both the c - ϕ natural soils and the cohesionless crusher run backfill were obtained using the log spiral earth pressure theory, modified for three-dimensional shape effects using Ovesen's (1964) procedure.

Pile cap resistance to horizontal movement is a function of the passive soil resistance developed at its front face, plus any sliding resistance on the sides and bottom of the cap, less any active earth pressure force on the back face of the cap. In the case of the bulkhead at Kentland Farms, the active force and the sliding resistance are small compared to the passive resistance, and they tend to offset each other. Passive earth pressure is thus the primary source of resistance to lateral load.

Conventional earth pressure theories consider only two-dimensional conditions, which correspond to a long wall moving against the soil. In the case of a bulkhead or pile cap, larger passive pressures are possible because of three-dimensional effects. A zone within the soil, which is wider than the face of the cap, is involved in resisting movement of the cap. The ratio between three-dimensional and two-dimensional soil resistance varies with the friction angle of the soil and the depth below the ground surface. Ovesen's theory provides a means of estimating the magnitude of this three-dimensional effect.

Ovesen (1964) conducted model tests on anchor blocks embedded in granular soils, and developed an empirical method for estimating the 3-D resistance of the embedded blocks.

Ovesen's expressions can be re-arranged to obtain a 3-D modifying factor (called R in this study) that can be calculated as follows:

$$R = 1 + (K_p - K_a)^{2/3} \left[1.1E^4 + \frac{1.6B}{1 + 5\frac{b}{H}} + \frac{0.4(K_p - K_a)E^3 B^2}{1 + 0.05\frac{b}{H}} \right] \quad \text{Equation 7.18}$$

where K_p and K_a are the passive and active earth pressure coefficients; b is the width of the cap measured horizontally in a direction normal to the applied load; H is the height of the cap; B is based on the spacing of multiple anchor blocks ($B = 1$ for a single pile cap); and E is based on the depth of embedment of the pile cap, defined as:

$$E = 1 - \frac{H}{z + H} \quad \text{Equation 7.19}$$

where z is the depth of embedment measured from the ground surface to the top of the cap.

The value of $K_{p\phi}$ determined in *PYCAP* is used in place of K_p in equation 7.11. K_a is determined using the Rankine earth pressure theory, which is approximately equivalent to the log spiral value because the active failure surface is very close to a plane.

The ultimate earth pressure force, P_{ult} (in units of force), can be determined by combining equations 7.12 and 7.18 as follows:

$$P_{ult} = RE_p b = R(P_{p\phi} + P_{pc} + P_{pq})b \quad \text{Equation 7.20}$$

where R is Ovesen's 3-D modifying factor (dimensionless), E_p is the two-dimensional or plane strain ultimate passive force (force per length units), b is the cap width or wall length (length units), $P_{p\phi}$ is the earth pressure component due to soil weight and friction (force per length units), P_{pc} is the earth pressure component due to cohesion (force per length units), P_{pq} is the earth pressure component due to surcharge (force per length units).

These calculations are performed in the worksheet named *Log Spiral*, which is part of the workbook *PYCAP*. A copy of the output generated by *PYCAP* is shown in Figure 7.21. This output was generated in the worksheet titled *Summary*, which is used for specifying soil parameters and cap dimensions, and for displaying calculated results, including pile cap p-y values. The p-y values are formatted for copying and pasting directly into *LPILE Plus 3.0* or *GROUP* data files. The *GROUP* p-y values are not shown in Figure 7.21. They are the same as the *LPILE Plus 3.0* values, except the p and y columns are transposed.

Ovesen's tests were performed on compacted sand with friction angles ranging from $\phi' = 32$ degrees to 41 degrees. The maximum difference in earth pressure coefficients ($K_p - K_a$) was 5.7 in Ovesen's tests, and R did not exceed a value of about 2. As a conservative measure, a limit of 2.0 was placed on the value of R that is calculated in *PYCAP*.

Using *PYCAP*, the passive resistance of the bulkhead was calculated for natural soils at the site and for crusher run gravel backfill. Estimated values of the average soil parameters at the center of the bulkhead were used in the analyses. Even though the applied load was horizontal, a small amount of wall friction developed as soil within the passive failure wedge moved upward, due to the weight of the bulkhead as it moved with the soil. The magnitude of the resulting frictional force is limited to the weight of the bulkhead, which is about 10 kips. This force corresponds to a wall friction angle, δ , of about 3.5 degrees for the natural soils, where the computed passive force was 160 kips, and $\delta = 6.2$ degrees for the crusher run gravel, where the computed passive force was 92 kips.

Average parameters for the natural soils were obtained from Figure 5.8 and consisted of $\phi = 37$ degrees, $c = 970$ psf, and $\gamma_m = 122$ pcf. For a wall friction angle of 3.5 degrees, $K_{p\phi} = 4.65$, $K_{pc} = 2.11$, $K_{pq} = 0$, and $K_a = 0.25$. Ovesen's R value was 1.43. Using these values, the calculated passive resistance, P_{ult} , was 160 kips for the bulkhead embedded in natural soil. As shown in Figure 7.20(a), the calculated ultimate resistance is in good agreement with the load test results. The *PYCAP* output sheet for this analysis shown in Figure 7.21

Parameters for the gravel backfill were determined using the data discussed in Chapter 5 and Appendix D. The measured ϕ' values for this material are very high at low confining pressures. ϕ' values as high as 53 degrees were determined at the center of the bulkhead, 1.75 feet below the ground surface. For these low confining pressures and high ϕ' values, some degree of progressive failure seems inevitable as a result of the sharply peaked stress-strain curves, as can be seen in Appendix D. As an allowance for these anticipated progressive failure effects, it was decided to use $\phi' = 50$ degrees for the compacted crusher run gravel.

For $\phi' = 50$ degrees, $c = 0$, $\gamma_m = 134$ pcf, and a wall friction angle of 6.2 degrees (corresponding to the weight of the bulkhead): $K_{p\phi} = 10.22$, $K_{pc} = K_{pq} = 0$, and $K_a = 0.13$. Ovesen's R value was 1.75. Using *PYCAP*, the calculated passive resistance, P_{ult} , was 92 kips for the bulkhead backfilled with crusher run gravel. As shown in Figure 7.20(b), the calculated ultimate resistance agrees quite well with the load test results, and is slightly conservative. The *PYCAP* output sheet for this analysis shown in Figure 7.22.

7.4.4 Pile Cap Stiffness

The initial stiffness of the pile cap response corresponds to the initial slope of the load deflection curve. This value can be approximated using elasticity theory. The approach by Douglas and Davis (1964) for estimating the horizontal displacement of a vertical rectangle in a semi-infinite homogenous elastic mass was used in this study. The slope of the calculated load versus elastic displacement curve is called k_{max} , which is defined as the initial elastic stiffness with units of force divided by length.

The approach used to estimate k_{max} is somewhat approximate in that it is based on the average deflection of the corners of a flexible rectangular area. This approach slightly underestimates the deflection because the deflection at the corners of a flexible area is smaller than the deflection of a rigid area, which would be a closer approximation of the bulkhead or of a pile cap. However, the difference between the average corner deflection for a flexible rectangle and the deflection of a rigid rectangle is offset by the effect of shear on the sides and bottom of the cap, which are neglected in the elastic solution. Thus, the use of an elastic

solution based on a flexible loaded area is approximate, but it is believed to be sufficiently accurate for practical purposes.

The parameters needed to estimate k_{\max} include Poisson's ratio (ν), the initial tangent modulus of the soil (E_i), and the dimensions and depth of the pile cap. A Poisson's ratio of 0.33 was assumed for the natural soils and a value of 0.30 was assumed for the granular backfill materials. The analysis is not sensitive to ν , and reasonable estimates can be obtained from published correlations based on type of soil, such as those shown in Table 7.3.

Estimates of the initial tangent modulus, E_i , were obtained from laboratory triaxial stress-strain curves, as described in Chapter 5. E_i values for the natural soils and backfill materials are shown in Figure 5.3. When triaxial data is unavailable, values of E_i can be estimated using published correlations. Table 7.4 contains typical ranges of E_i for various types of soil, and Table 7.5 contains equations that can be used to calculate E_i based on in situ test results for coarse-grained soils, or undrained shear strengths (S_u) for fine-grained soils.

The equations used to compute k_{\max} are given in Appendix H. These equations and associated influence factors are programmed in the worksheet called *Elasticity*, which is part of the *PYCAP* workbook. Figure 7.23 contains an example of the *Elasticity* worksheet that was used to compute k_{\max} for the natural soils. k_{\max} calculations are performed automatically when the *Summary* worksheet is activated. It is not necessary to enter the worksheet *Elasticity* to calculate pile cap p-y values, because the required soil parameters and cap dimensions are input in the *Summary* worksheet. The results, including the calculated k_{\max} value, are also displayed in the *Summary* worksheet.

Using this approach, values of k_{\max} were computed for the bulkhead embedded in natural soil ($k_{\max} = 890$ kips/in) and for the bulkhead embedded in compacted gravel ($k_{\max} = 760$ kips/in).

7.4.5 Pile Cap p-y Curves

Load-deflection curves for the pile caps and bulkhead were estimated using a hyperbolic equation of the same form as used by Duncan and Chang (1970) to represent stress-strain curves for soil. The hyperbolic load-deflection relationship is expressed as:

$$P = \frac{y}{\left(\frac{1}{k_{\max}} + R_f \frac{y}{P_{ult}} \right)} \quad \text{Equation 7.21}$$

where P is the load at any deflection y , P_{ult} is the ultimate passive force (Section 7.4.2), k_{\max} is the initial stiffness (Section 7.4.4), and R_f is the failure ratio. The failure ratio is defined as the ratio between the actual failure force and the hyperbolic ultimate force, which is an asymptotic value that is approached as y approaches infinity. For soil stress-strain curves, R_f is always smaller than unity, and varies from 0.5 to 0.9 for most soils (Duncan et al. 1980). The value of R_f can be estimated by substituting P_{ult} for P , and by substituting the movement required to fully mobilize passive resistance, Δ_{\max} , for y . Re-arranging the terms in Equation 7.21 results in the following expression for R_f :

$$R_f = 1 - \frac{P_{ult}}{\Delta_{\max} k_{\max}} \quad \text{Equation 7.22}$$

Calculations for R_f are performed in the *PYCAP* worksheet called *Hyperbola* using Equation 7.22. A copy of the *Hyperbola* worksheet is shown in Figure 7.24, for the bulkhead embedded in natural soil. Based on finite element and experimental studies by Clough and Duncan (1971), Δ_{\max} was assumed to equal 4 % of the wall (or cap) height for the foundations in this study. As shown in Table 7.6, the value of R_f calculated using Equation 7.22 ranged from 0.67 to 0.97 for the pile caps and bulkhead at the Kentland Farms test facility, with an average value of 0.83.

Using Equation 7.21 with the values of P_{ult} and k_{\max} described in the previous sections, load versus deflection curves were computed for the bulkhead. Calculated results are

compared to observed responses for the bulkhead in natural soil (Figure 7.25a) and for the bulkhead backfilled with gravel (Figure 7.25b). As shown in the plots, the calculated results are in good agreement with the measured response curves over the full range of deflections.

Calculated load-deflection curves can readily be converted to p-y curves by dividing the load, P , by the cap height. This approach results in a constant value of resistance versus depth. A linear variation can also be assumed, but the difference between a constant value and a linear variation is negligible. Consequently, a constant value was assumed in the analyses conducted for this study.

All the components necessary for calculating pile cap p-y values have been described in the preceding pages. Soil parameters and cap dimensions are input in the *Summary* worksheet, P_{ult} is calculated in the *Log Spiral* worksheet, and k_{max} is calculated in the *Hyperbolic* worksheet. The hyperbolic equation is solved and p-y values are calculated in the *Hyperbolic* worksheet, and the output is displayed in the *Summary* worksheet.

Based on the approach described in this section, the computer spreadsheet named *PYCAP* was developed for calculating pile cap p-y curves. *PYCAP* includes the worksheets *Summary*, *Log Spiral*, *Hyperbola*, *Elasticity*, and *PYPILE*. (*PYPILE* is used to compute p-y curves for piles rather than caps, and works independently of the other sheets.) The cap p-y values are formatted for copying and pasting from the *Summary* worksheet directly into an *LPILE Plus3.0* or *GROUP* data input file. Computed results, such as the earth pressure coefficients (Rankine, Coulomb, and log spiral), Ovesen's 3-D factor (R), k_{max} , and P_{ult} are displayed in the *Summary* worksheet. An example of p-y curves calculated for the 36-in-deep cap in natural soil, compacted gravel, compacted sand, and loose sand are shown in Figure 7.26. The parameters used to develop the cap p-y curves are summarized in Table 7.7. A metric (or SI) units version of the *PYCAP* worksheet was also created, called *PYCAPSI*. *PYCAPSI* has all the same features as *PYCAP*, except SI units are used for the data and the computations.

The components necessary for creating soil models for pile groups and pile caps were described in the previous sections. These models, in the form of p-y curves, can be input into computer programs such as *LPILE Plus 3.0* (1997), *GROUP* (1996), or *Florida Pier* (1998) to compute the lateral response of the foundation system. *GROUP* and *Florida Pier* contain matrix structural analysis packages for computing reactions that are caused by interactions between the piles and pile cap. However, numerous problems were encountered when externally generated pile cap p-y curves were used with these programs, and it appears that they require further development and validation before they can be used with cap resistance.

For this reason, the simplified method described previously was developed for use in *LPILE Plus 3.0*. This method models the pile group as a “group-equivalent pile” (abbreviated GEP), with a rotationally restrained pile head boundary condition. The pile cap is modeled as an enlarged section with pile cap p-y values from *PYCAP*. This approach has been used to calculate the load-deflection responses of the foundations tested in this study. The results of the analyses are described in the following section.

7.5 COMPARISON OF MEASURED AND CALCULATED LOAD-DEFLECTION RESULTS

7.5.1 Background

Load-deflection response curves were calculated for the 3 pile groups described in Chapter 6. The response curves were developed for pile caps embedded in natural soil, and for pile caps backfilled with granular material (crusher run gravel or New Castle sand). The analyses were performed using the following procedure:

1. **Estimate soil parameters** (Chapter 5). Values are listed in Figure 5.8 for the natural soil and Table 5.9 for the granular backfill.
2. **Calculate single pile p-y curve** (Section 7.2). For c- ϕ soils, use Brinch-Hansen’s ultimate theory together with

the cubic parabola formulation for p-y curves. This is done in the spreadsheet *PYPILE*.

3. **Modify the single pile curve for group effects** (Section 7.3.2). The “group-equivalent pile” p-y curves are developed in *PYPILE* by multiplying the p-values by the term $\sum_{i=1}^N f_{mi}$. Values of f_m can be obtained from Figure 2.15. The “group-equivalent pile” p-y curves can be copied and pasted from *PYPILE* directly into *LPILE Plus 3.0*.
4. **Estimate the pile-head rotational restraint** (Section 7.3.4). Evaluate $k_{m\theta}$ based on the axial capacities of the piles and their spacings in the group.
5. **Determine P_{ult} for the pile cap** (Section 7.4.3). Use the log spiral earth pressure theory in conjunction with Ovesen’s 3-D factor. Calculation are performed using *PYCAP*.
6. **Determine the initial cap stiffness, k_{max}** (Section 7.4.4). Use elasticity theory by Douglas and Davis (1964). Calculation are performed using *PYCAP*.
7. **Develop p-y curves for the pile cap** (Section 7.4.5). Use the hyperbolic formulation with P_{ult} and k_{max} . The cap p-y curves can be copied and pasted from the spreadsheet *PYCAP* directly into *LPILE Plus 3.0*.
8. **Perform the analysis** (use *LPILE Plus 3.0*). Analyze the load-deflection behavior of the “group-equivalent pile”

(GEP) to determine deflections, moments, and shear forces for the pile group.

Steps 2 through 7 are automated in the spreadsheet *PYCAP*. Step 8 can be performed using lateral analysis computer programs such as *LPILE Plus 3.0*, *GROUP*, or *Florida Pier*. The analyses conducted during this study were performed using the GEP approach with *LPILE Plus 3.0*. The input parameters that were used to calculate pile cap p-y values are summarized in Table 7.7.

The procedure outlined above was used to calculate load-deflection curves for the three pile groups at the Kentland Farms test facility. These curves were compared to the observed responses measured during the load tests, as described in the following sections.

7.5.2 Pile Caps Embedded in Natural Soil

Analyses were performed for the NE, NW, and SE pile groups with their caps embedded in natural soils. These caps were constructed by pouring concrete against undisturbed natural ground. Intimate, uniform contact was achieved between the cap and natural soil, thus, a relatively high value of wall friction ($\delta = 0.8\phi$) was assumed. The values of soil parameters that were used in the analyses are shown in Table 7.7. Calculated load-deflection plots are compared to measured response curves in Figure 7.27. The k_{m0} values used in the analyses are shown in the plots. Details pertaining to these values are described in Section 7.3.4.

As shown in the plots in Figure 7.27, the calculated deflections for the three groups were larger than the measured responses and are therefore somewhat conservative. The discrepancy between calculated and measured deflections indicates that the strength of the natural soil in the top 3 feet may have been underestimated. This soil was highly desiccated, making it difficult to obtain undisturbed samples, even using block sampling techniques. Consequently, the triaxial strength tests may have resulted in estimates of shear strength that are smaller than the actual in situ strengths, because of sample disturbance.

The difference between observed and calculated results could also be affected by construction-related factors that are difficult to account for in any analytical method. For example, the method of cap construction can affect the rotational stiffness of the system. The caps were constructed at this test facility by pouring concrete against carefully excavated, undisturbed trench sidewalls. Consequently, cap rotations were probably less than the calculated values. This may explain, in part, the conservative nature of the calculated response curves shown in Figure 7.27.

7.5.3 Pile Caps Backfilled with Granular Backfill

Load tests were performed on the NE, NW, and SE pile caps backfilled with compacted crusher run gravel. The SE cap was also tested using uncompacted and compacted New Castle sand backfill. A comprehensive laboratory program was conducted to develop soil parameters for the backfill materials, based on measured field densities. These parameters are described in Chapter 5. The soil parameters used in the analyses are summarized in Table 7.7.

The backfill was placed and compacted around the caps after the natural soil was excavated and removed. During construction, backfill along the cap face was most likely not compacted as well as the backfill in the remainder of the excavation because of difficulties in compacting immediately adjacent to the vertical concrete face. For this reason, the wall friction angle, δ , was assumed equal to 0.5ϕ .

Results calculated using *PYCAP* are shown in Table 7.6. Calculated load-deflection curves are compared to measured results in Figure 7.28 for the pile caps backfilled with gravel, and in Figure 7.29 for the SE cap backfilled with sand.

As shown in Figures 7.28 and 7.29, the agreement between measured and calculated results is quite good for the pile caps in granular backfill. For the most part, the differences between calculated and observed deflections were less than 30 %. In the case of the NW cap, the calculated load-deflection curve is virtually identical to the measured response (Figure

7.28b). The calculated results are conservative in all cases except the SE cap backfilled with New Castle sand. In this case, the calculated deflections are greater than the observed deflections at loads below 70 kips, and the calculated deflections are less than the observed deflection at loads above 70 kips (Figure 7.29).

7.6 COMPARISONS WITH RESULTS OF LOAD TESTS PERFORMED BY OTHERS

7.6.1 Background

Four studies were described in Chapter 2 in which the responses of pile groups with and without cap resistance were compared. The analytical approach described in the previous sections of this chapter was used to analyze foundation responses for the Zafir and Vanderpool (1998) load tests. The study by Beatty (1970) did not contain sufficient information regarding soil conditions and foundation size. The study by Rollins et al. (1997) was excluded because a rapid impact loading was used in their test. Kim and Sing's (1974) work was excluded because the pile cap was not embedded in their study, but was constructed on the ground surface and was not backfilled.

7.6.2 Zafir and Vanderpool (1998) Case Study

The load tests reported by Zafir and Vanderpool (1998) were associated with a construction project at a new interstate interchange (I-15/US95) in Las Vegas, Nevada. The pile group consisted of four 2-foot-diameter drilled shafts, each 33 feet long, and spaced at 2D center to center. The cap consisted of an 11-foot-diameter reinforced cap, drilled to a depth of about 10 feet. Subsurface conditions at the site consisted of interlayers of sandy clay, silty clay, and clayey sand. Very stiff caliche deposits occurred at depths of 14 to 18.5 feet and 35 to 38 feet. Groundwater was reported at 13 feet below the ground surface. Soil parameters used to perform the analyses were obtained from Zafir and Vanderpool's (1998) report, and are shown in Table 7.8.

Group-equivalent pile (GEP) p-y curves were developed using the procedure described in Section 7.2 with the spreadsheet *PYPILE* and the soil parameters shown in Table 7.8. p-y curves for the stiff clay layers are shown in Figure 7.30(a), and p-y curves for the caliche layers are shown in Figure 7.30(b). Pile cap soil resistance was modeled using cap p-y curves calculated using *PYCAP*. The *PYCAP Summary* worksheet for this analysis is shown in Figure 7.31. The cap resistance versus deflection relationship (p-y curve) was developed for a calculated ultimate passive force, P_{ult} , of 1096 kips and an initial elastic stiffness, k_{max} , of 6700 kips/in. The cap p-y curve is shown in Figure 7.30(a).

Three boundary conditions were used in the analyses: fixed-head (zero rotation), free-head (zero moment), and rotationally restrained ($k_{m\theta}$ value) pile head. As shown in Figure 7.32(a), the calculated response based on a fixed-head boundary condition underestimated the observed deflection by approximately 90 %, at a load of 1500 kips. In contrast, the calculated deflection based on a free-head boundary condition was over-conservative by over 300 %.

Excellent agreement between calculated and observed load-deflection response was obtained by assuming a rotationally restrained pile-head boundary condition, as shown in Figure 7.32(b). Pile-head rotational stiffness was estimated using $k_{m\theta}$ calculated from Equation 7.11. A value of $k_{m\theta} = 1.93 \times 10^{10}$ in-lb/rad was determined based on an estimated skin friction, Q_s , of 262 tons per pile, mobilized at a vertical movement of 0.1 inches. The ultimate bending moment resisting cap rotation, M_{ult} , was estimated to be 4200 ft-kips. The measured response was well predicted by the analytical approach. The plots in Figure 7.32 demonstrate the importance of pile-head boundary conditions in the analyses.

7.7 SUMMARY OF DESIGN METHOD

The preceding sections describe the details of the approach developed for analyzing laterally loaded pile groups. The approach can be summarized in a step-by-step design method, as described below.

Step 1. Estimate soil parameters.

The soil parameters required for the analyses are: ϕ , c , δ , α , ν , E_i , and γ_m .

Undrained (total stress) values of ϕ and c should be used for fine-grained soils. These values can be obtained from UU triaxial tests or estimated using correlations with in situ test results, such as those obtained from SPT, CPT or vane shear tests. Drained (effective stress) values should be used for cohesionless soils. Values of ϕ' can be estimated using correlations with in situ test results, such as SPT or CPT, or by performing CD triaxial tests. c' is usually assumed equal to zero for effective stress analyses. Figure 7.33 or other correlations can be used to approximate ϕ' if the soil type and relative density, or dry unit weight are known..

Wall friction, δ , and the adhesion factor, α , can be estimated based on type of soil and type of interface material using Table 7.1 and Table 7.2, respectively.

Poisson's ratio can be estimated from correlations based on type of soil (Table 7.3).

Values of initial tangent modulus, E_i , can be obtained using stress-strain results from triaxial tests or estimated based on type of soil (Table 7.4) or based on SPT N values, CPT q_c values, or S_u values (Table 7.5).

Soil unit weight, γ_m , can be measured in the lab or estimated from correlations based on type of soil and relative density or consistency (see Figure 7.33).

Step 2. Calculate single pile p-y curves.

For c - ϕ soils, use Brinch-Hansen's ultimate theory together with the cubic parabola formulation to develop p-y curves. This is done in the spreadsheet *PYPILE*, which is a separate worksheet in *PYCAP*. *PYPILE* can also be used for $c = 0$ or for $\phi = 0$ soils, or the "default" p-y formulations in *LPILE Plus 3.0* can be used. (Step 2 is discussed in Section 7.2.)

Step 3. Modify the single pile p-y curves for group effects.

The group-equivalent pile (GEP) p-y curves are developed in *PYPILE* by multiplying the p-values by the term $\sum_{i=1}^N f_{mi}$. Values of f_m can be obtained from Figure 2.15. The GEP p-y curves can be copied and pasted from *PYPILE* directly into *LPILE Plus 3.0*. (Step 3 is discussed in Section 7.3.2.)

Step 4. Estimate the pile-head rotational restraint, $k_{m\theta}$.

The rotational restraint is a function of the side resistance of the piles, the deflection required to mobilize skin friction, and the corresponding moment on the pile cap. $k_{m\theta}$ is determined using Equation 7.11. The pile skin friction capacity, Q_{si} , can be calculated using rational approaches such as the α -method (Tomlinson 1987), β -method (Esrig and Kirby 1979) and the λ -method (Vijayvergiya and Focht 1972). In situ approaches are also available, such as the SPT method developed by Meyerhof (1976) or the CPT method by Nottingham and Schmertmann (1975). The computer program *SPILE* (1993), available from the FHWA, is useful for computing values of Q_{si} . (Step 4 is discussed in Section 7.3.4.)

Step 5. Determine P_{ult} for the pile cap.

The ultimate lateral load resistance of the pile cap is determined using the log spiral earth pressure theory and Ovesen's 3-D correction factor. Calculations for P_{ult} are performed using the *EXCEL* workbook named *PYCAP*. *PYCAP* contains the worksheets *Summary*, *Log Spiral*, *Hyperbola*, *Elasticity*, and *PYPILE*. Soil parameters and cap dimensions are specified in worksheet *Summary*. P_{ult} calculations are performed in worksheet *Log Spiral*. The results are displayed in the *Summary* worksheet. (Step 5 is discussed in Section 7.4.3, and the log spiral theory is described in Appendix F.)

Step 6. Determine the cap stiffness, k_{max} .

The initial stiffness of the pile cap is approximated using elasticity theory. k_{max} is calculated using the worksheet *Elasticity*, which is part of the *PYCAP* workbook. Soil parameters needed for k_{max} calculations (E_i and ν) and cap dimensions are specified in the

Summary worksheet. Calculations for k_{\max} are performed automatically when worksheet *Summary* is activated. (Step 5 is discussed in Section 7.4.4, and the elastic equations used in the *Elasticity* worksheet are described in Appendix H.).

Step 7. Develop p-y curves for the pile cap

Pile cap p-y values are developed using the hyperbolic formulation with P_{ult} and k_{\max} . Parameters are specified in the *Summary* worksheet, calculations are performed in the *Hyperbolic* worksheet, and the results, p-y values, are displayed in the *Summary* worksheet. The cap p-y values can be copied and pasted from the *Summary* worksheet directly into *LPILE Plus 3.0*. (Step 7 is discussed in Section 7.4.5.)

Step 8. Perform the analysis.

The lateral response of the pile group is analyzed using *LPILE Plus 3.0*. p-y curves developed for the GEP (Step 3) and for the pile cap (Step 7) are used to represent the soil resistance. The pile group is modeled as a single pile with EI equal to the sum of the EI values for all of the piles in the group. The cap is modeled by enlarging the top portion of the GEP based on the cap dimensions. A rotationally restrained pile-head boundary condition is specified using the value of $k_{m\theta}$ calculated during Step 6.

Step 9. Evaluate the results.

The calculated displacements of the GEP correspond to the displacements of the actual pile group. However, to determine the shear forces (V) and moments (M) of the piles within the group, the shear forces and moments of the GEP are factored based on the pile's row multiplier, f_{mi} and the EI value for each pile. This is done as follows:

$$V_i = V_{\text{gep}} \left(\frac{f_{mi} EI_i}{\sum_{i=1}^N (f_{mi} EI_i)} \right) (f_{mc}) \quad \text{Equation 7.22}$$

where V_i is the shear in pile i , V_{gep} is the total shear for the GEP, N is the number of piles, f_{mi} is the p -multiplier for the row containing the pile of interest (f_m is obtained from Figure 2.15), EI_i is the flexural stiffness of pile i , and f_{mc} is a multiplier for corner piles. Corner piles in the leading row carry a larger share of the load than non-corner piles. Consequently, the corner piles will have larger shear forces and bending moments. The multiplier, f_{mc} , is an adjustment factor to account for larger values of V_i and M_i in the corner piles. Based on 1g model tests by Franke (1988), the following values are recommended for f_{mc} :

| Pile spacing measured normal to direction of load | f_{mc} factor |
|--|-----------------|
| non-corner piles | 1.0 |
| $\geq 3D$ | 1.0 |
| $2D$ | 1.2 |
| $1D$ | 1.6 |

The moment in pile i is computed as:

$$M_i = M_{\text{gep}} \left(\frac{f_{mi} EI_i}{\sum_{i=1}^N (f_{mi} EI_i)} \right) (f_{mc}) \quad \text{Equation 7.23}$$

where M_i is the moment in pile i and M_{gep} is the moment computed for the GEP.

Equations 7.22 and 7.23 can be simplified using a distribution coefficient called D_i , which is defined as:

$$D_i = \left(\frac{f_{mi} EI_i}{\sum_{i=1}^N (f_{mi} EI_i)} \right) \quad \text{Equation 7.24}$$

Thus, the shear and moment in pile i are determined using the following equations:

$$V_i = V_{gep} D_i f_{mc} \quad \text{Equation 7.25a}$$

$$M_i = M_{gep} D_i f_{mc} \quad \text{Equation 7.25b}$$

7.8 SUMMARY

An analytical approach was developed for evaluating the lateral response of pile groups with embedded caps. The approach involves creating p-y curves for single piles, pile groups, and pile caps using the computer spreadsheets *PYPILE* and *PYCAP*.

Single pile p-y curves are developed using Brinch Hansen's (1961) ultimate load theory for soils that possess both cohesion and friction. The approach is programmed in *PYPILE*, which can be used to calculate p-y curves for piles of any size, with soil properties that are constant or that vary with depth.

"Group-equivalent pile" (abbreviated GEP) p-y curves are obtained by multiplying the "p" values of the single pile p-y curves by a modification factor that accounts for reduced capacities caused by group interaction effects, and summing the modified p-values for all the piles in the group. The p-multiplier curves developed in Chapter 2 are used for this purpose. The pile group is modeled in the computer program *LPILE Plus 3.0* using these GEP p-y curves. The flexural resistance of the GEP pile is equal to the sum of the flexural resistances of all the piles in the group.

A rotationally restrained pile-head boundary condition is used in the analysis. The rotational stiffness is estimated from the axial skin friction of the piles, the deflection required to mobilize skin friction, and the corresponding moment on the pile cap.

Pile cap resistance is included in the analysis using cap p-y curves. A method of calculating cap p-y curves was developed during this study, and has been programmed in the spreadsheet *PYCAP*. The approach models the passive earth pressures developed in front of the cap. These passive pressures are represented by p-y curves developed from a modified hyperbolic formulation, which is defined by the ultimate passive force and the initial elastic stiffness of the embedded pile cap. The ultimate passive force is determined using the log spiral earth pressure theory in conjunction with Ovesen's (1964) three-dimensional correction factors.

The GEP approach for creating pile group and pile cap p-y curves provides a means of modeling the soil in a way that is compatible with established approaches for analyzing laterally loaded single piles. *LPILE Plus 3.0* was used to calculate load-deflection curves for the pile groups tested in this study, and for a load test described in the literature. Comparisons between measured and calculated load-deflection responses indicate that the analytical approach developed in this study is conservative, reasonably accurate, and suitable for design purposes. Deviations between calculated and measured load-deflection values fall well within the practical range that could be expected for analyses of the lateral response of pile groups. This approach represents a significant improvement over current design practices, which often completely ignore the cap resistance.

The author believes it would be difficult to obtain more accurate estimates of pile group behavior, even with more complex analytical methods, because of the inevitable uncertainties and variations in soil conditions, unknown or uncontrollable construction factors, and the complex structural and material interactions that occur between the piles, pile cap, and soil.

Table 7.1. Friction angles, δ , between various soils and foundation materials (After NAVFAC, 1982.)

| Interface material | Friction angle, δ (degrees) |
|--|---------------------------------------|
| <i>Mass concrete or masonry on the following soils:</i> | |
| clean sound rock | 35 |
| clean gravel, gravel-sand mixtures, coarse sand | 39 to 31 |
| clean fine to medium sand, silty medium to coarse sand, silty or clayey gravel | 24 to 29 |
| fine sandy silt, nonplastic silt | 17 to 19 |
| very stiff and hard residual or preconsolidated clay | 22 to 26 |
| medium stiff and stiff clay and silty sand | 17 to 19 |
| <i>Formed concrete or concrete sheet piling against the following soils:</i> | |
| clean gravel, gravel-sand mixtures, well-graded rock fill with spalls | 22 to 26 |
| clean sand, silty sand-gravel mixture, single size hard rock fill | 17 to 22 |
| silty sand, gravel or sand mixed with silt or clay | 17 |
| fine sandy silt, nonplastic silt | 14 |

Table 7.2. Typical values of the soil adhesion factor, α . (After NAVFAC, 1982.)

| Interface soil | Soil cohesion c (psf) | Adhesion factor α |
|----------------------------|----------------------------------|---|
| Very soft cohesive soil | 0 to 250 | 1.0 |
| Soft cohesive soil | 250 to 500 | 1.0 |
| Medium stiff cohesive soil | 500 to 1000 | 1.0 to 0.75 |
| Stiff cohesive soil | 1000 to 2000 | 0.75 to 0.5 |
| Very stiff cohesive soil | 2000 to 4000 | 0.5 to 0.3 |

Table 7.3. Typical range of values for Poisson's ratio. (After Bowles, 1982.)

| Type of soil | Poisson's ratio, μ |
|--|------------------------|
| Sand (dense) | 0.2 to 0.4 |
| coarse-grained (void ratio = 0.4 to 0.7) | 0.15 |
| fine-grained (void ratio = 0.4 to 0.7) | 0.25 |
| Silt | 0.3 to 0.35 |
| Loess | 0.1 to 0.3 |
| Sandy Clay | 0.2 to 0.3 |
| Clay | |
| saturated | 0.4 to 0.5 |
| unsaturated | 0.1 to 0.3 |
| Rock (depends on rock type) | 0.1 to 0.4 |
| Concrete | 0.15 |
| Ice | 0.36 |

Table 7.4. Typical range of E_i values for various soil types. (After Bowles, 1982.)

| Type of soil | E_i | |
|-----------------|------------------|---------------|
| | (ksf) | (Mpa) |
| Sand | | |
| silty | 150 to 450 | 7 to 21 |
| loose | 200 to 500 | 10 to 24 |
| dense | 1000 to 1700 | 48 to 81 |
| Sand and Gravel | | |
| loose | 1000 to 3000 | 48 to 144 |
| dense | 2000 to 4000 | 96 to 192 |
| Glacial Till | | |
| loose | 200 to 3200 | 10 to 153 |
| dense | 3000 to 15,000 | 144 to 720 |
| very dense | 10,000 to 30,000 | 478 to 1440 |
| Silt | 40 to 400 | 2 to 20 |
| Loess | 300 to 1200 | 14 to 57 |
| Clay | | |
| very soft | 50 to 250 | 2 to 15 |
| soft | 100 to 500 | 5 to 25 |
| medium | 300 to 1000 | 15 to 50 |
| hard | 1000 to 2000 | 50 to 100 |
| sandy | 500 to 5000 | 25 to 250 |
| Shale | 3000 to 300,000 | 144 to 14,400 |
| Silt | 40 to 400 | 2 to 20 |

Table 7.5. Equations for E_i by several test methods. (After Bowles, 1982.)

| Type of soil | SPT (E_i in units of ksf) | CPT (E_i in units of q_c) | Undrained shear strength, S_u (E_i in units of S_u) |
|-------------------------------|---|---|---|
| sand | $E_i = 100(N + 15)$ $E_i = 360 + 15N$ $E_i = (300 \text{ to } 440)\ln(N)$ | $E_i = (2 \text{ to } 4)q_c$ $E_i = 2(1 + D_r^2)q_c$ | |
| clayey sand | $E_i = 6.4(N + 15)$ | $E_i = (3 \text{ to } 6)q_c$ | |
| silty sand | $E_i = 6(N + 6)$ | $E_i = (1 \text{ to } 2)q_c$ | |
| gravelly sand | $E_i = 24(N + 6)$ | | |
| soft clay | | $E_i = (6 \text{ to } 8)q_c$ | |
| clay, $PI > 30$ or organic | | | $E_i = (100 \text{ to } 500)S_u$ |
| clay, $PI < 30$ or stiff | | | $E_i = (500 \text{ to } 1500)S_u$ |
| clay, $1 < OCR < 2$ | | | $E_i = (800 \text{ to } 1200)S_u$ |
| clay, $OCR > 2$ | | | $E_i = (1500 \text{ to } 2000)S_u$ |

Notes:

1. Multiply ksf by 47.88 to obtain E_i in units of kPa.
2. q_c = cone penetrometer (CPT) tip resistance
3. D_r = relative density
4. PI = plasticity index = $LL - PL$
5. OCR = overconsolidation ratio
6. S_u = undrained shear strength

Table 7.6. Summary of results from *PYCAP* analyses.

| Foundation | Soil around pile cap | Hyperbolic R_f | K_{pf} | K_{pc} | K_{pq} | 3-D factor R | k_{max} (kips/inch) | P_{ult} (kips) |
|----------------|----------------------|------------------|----------|----------|----------|----------------|-----------------------|------------------|
| Bulkhead | natural soil | 0.89 | 4.65 | 2.11 | 0 | 1.43 | 891 | 160 |
| Bulkhead | gravel backfill | 0.93 | 10.22 | 0 | 0 | 1.75 | 756 | 92 |
| NE 36-inch cap | natural soil | 0.70 | 12.51 | 4.42 | 0 | 1.91 | 733 | 322 |
| NE 36-inch cap | gravel backfill | 0.82 | 26.46 | 0 | 0 | 2.00 | 623 | 160 |
| NW 18-inch cap | natural soil | 0.67 | 12.71 | 4.41 | 7.66 | 1.87 | 619 | 148 |
| NW 18-inch cap | gravel backfill | 0.89 | 26.46 | 0 | 0 | 1.80 | 462 | 36 |
| SE 36-inch cap | natural soil | 0.70 | 12.51 | 4.42 | 0 | 1.91 | 733 | 322 |
| SE 36-inch cap | gravel backfill | 0.82 | 26.46 | 0 | 0 | 2.00 | 623 | 160 |
| SE 36-inch cap | compacted sand | 0.95 | 16.92 | 0 | 0 | 2.00 | 1147 | 79 |
| SE 36-inch cap | loose sand | 0.97 | 7.58 | 0 | 0 | 1.65 | 590 | 26 |

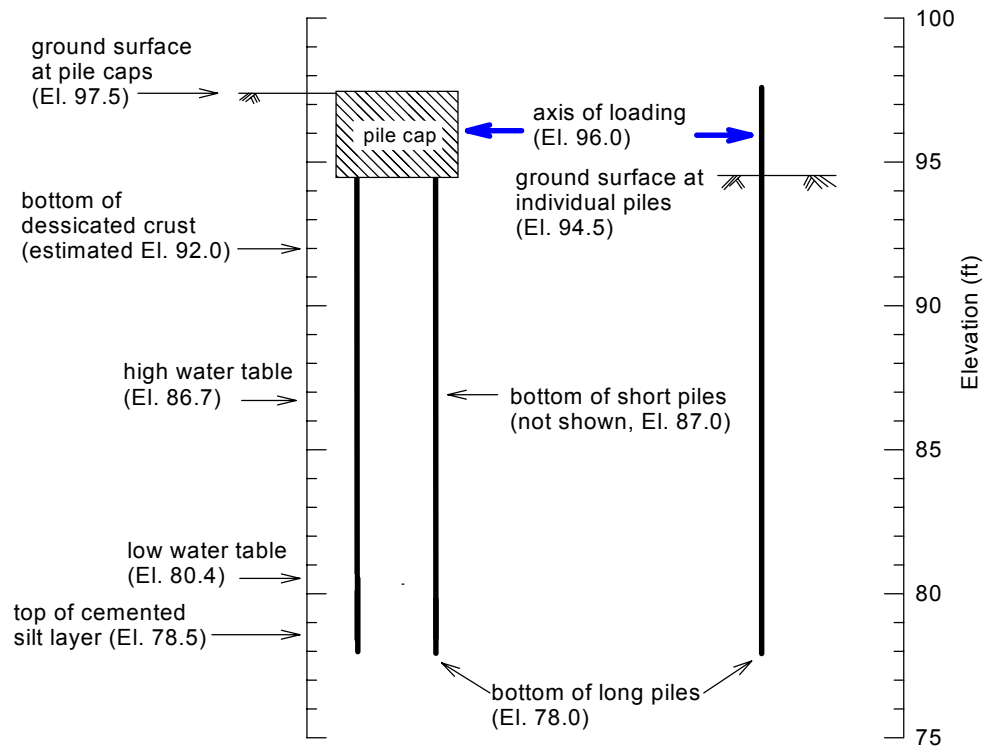
Table 7.7. Parameters used to calculate pile cap p-y curves.

| Parameter | Natural soil | Compacted gravel | Compacted sand | Loose sand |
|------------------|--------------|------------------|----------------|------------|
| ϕ (deg) | 38 | 50 | 46 | 37 |
| δ (deg) | 30 | 25 | 23 | 18.5 |
| c (psi) | 7 | 0 | 0 | 0 |
| α | 1 | 0 | 0 | 0 |
| γ_m (pcf) | 123 | 134 | 104 | 92 |
| E_i (ksf) | 890 | 760 | 1400 | 720 |
| ν | 0.33 | 0.30 | 0.30 | 0.30 |

Table 7.8. Soil parameters used in the Zafir and Vanderpool case study.

| Depth (ft) | Soil type | \bar{g} (pcf) | k (pci) | S_u (psf) | e_{50} |
|---------------|------------|--------------------|--------------|----------------|----------|
| 0.0 to 10.0 | stiff clay | 125 | 1,000 | 3,000 | 0.0050 |
| 10.0 to 14.0 | stiff clay | 120 | 600 | 1,300 | 0.0066 |
| 14.0 to 18.5 | caliche | 140 | > 2,000 | 566,000 | 0.0010 |
| 18.5 to 35.0 | stiff clay | 125 | 2,000 | 6,000 | 0.0040 |
| 35.0 to 38.0 | caliche | 140 | > 2,000 | 560,000 | 0.0005 |

Note: The parameters shown in this table were obtained from Zafir and Vanderpool's (1998) report.



| Elevation (ft) | Moist unit weight, γ_m (pcf) | Cohesion total stress, c (psi) | Friction angle total stress, ϕ (degrees) | Strain at 50% σ_{dmax} ϵ_{50} |
|----------------|-------------------------------------|----------------------------------|---|---|
| 97.5 | 123.7 | 7.0 | 38.0 | 0.01 |
| 96.0 | 122.8 | 7.0 | 38.0 | 0.01 |
| 94.5 | 121.9 | 7.0 | 38.0 | 0.01 |
| 92.0 | 120.4 | 6.0 | 35.0 | 0.025 |
| 88.0 | 118.0 | 5.0 | 28.0 | 0.025 |
| 87.0 | 117.4 | 4.3 | 27.0 | 0.025 |
| 80.0 | 112.4 | 4.0 | 25.0 | 0.025 |
| 79.0 | 112.3 | 0.0 | 45.0 | 0.002 |
| 78.0 | 112.0 | 0.0 | 45.0 | 0.002 |

Figure 7.1. Soil parameters for calculating p-y curves.

Soil Resistance vs. Deflection (p-y) Calculation Sheet for Single Pile

Date: 8/9/99
 Project: Single pile natural soil
 Engineer: rlm

| | | Input (red lettering) | | | | | | Calculated Values | | |
|--------------------------|--------|-----------------------|---------|--------------|-----------------|-----|------|----------------------|-------|-------------------|
| Slope Angle (deg), $i =$ | | 0 | | | | | | Brinch-Hansen (1961) | | |
| Depth, x (ft) | D (ft) | γ (pcf) | c (psf) | ϕ (deg) | ϵ_{50} | A | M | K_c | K_q | p_{ult} (lb/in) |
| 0.00 | 0.83 | 121.9 | 1008 | 38 | 0.01 | 2.5 | 0.85 | 10.57 | 9.07 | 626 |
| 2.50 | 0.83 | 120.4 | 864 | 35 | 0.01 | 2.5 | 0.85 | 42.13 | 11.87 | 2,350 |
| 6.50 | 0.83 | 118 | 720 | 28 | 0.025 | 2.5 | 0.85 | 34.93 | 8.87 | 1,879 |
| 14.50 | 0.83 | 50 | 576 | 25 | 0.025 | 2 | 0.85 | 31.84 | 8.01 | 1,420 |
| 15.50 | 0.83 | 50 | 0 | 45 | 0.002 | 2.5 | 0.85 | 344.75 | 72.66 | 3,311 |
| 16.50 | 0.83 | 50 | 0 | 45 | 0.02 | 2.5 | 0.85 | 356.23 | 75.21 | 3,648 |
| 0.00 | 0 | 0 | 0 | 0 | 0.02 | 2.5 | 0.85 | #DIV/0! | 0.00 | #DIV/0! |
| 0.00 | 0 | 0 | 0 | 0 | 0.002 | 2.5 | 0.85 | #DIV/0! | 0.00 | #DIV/0! |
| 0.0 | 0 | 0 | 0 | 0 | 0.002 | 2.5 | 0.85 | #DIV/0! | 0.00 | #DIV/0! |

| Definition of Parameters | | | |
|--------------------------|--|-------------|---|
| x = | depth below ground surface (ft) | K_c = | cohesive resistance coefficient |
| D = | shaft diameter (ft) | K_q = | friction resistance coefficient |
| γ = | soil unit weight (pcf) | p_{ult} = | ultimate soil resistance (in-lb/in ²) |
| c = | soil cohesion (psf) | p = | soil resistance (in-lb/in ²) |
| ϕ = | soil friction angle (deg) | y = | shaft deflection |
| ϵ_{50} = | strain required to mobilize 50% of the soil strength | | |
| A = | p-y curve shape factor | | |
| M = | ultimate lateral load reduction factor | | |

The p-y values calculated below (shaded cells) are formatted for cutting and pasting directly into LPILE plus 3.0 input files.

| Brinch-Hansen p-y values | | | |
|--------------------------|-------------|--------|-----------|
| Depth (in) | p/p_{ult} | y (in) | p (lb/in) |
| 0.0 | 0.000 | 0.0 | 10 |
| 0.1 | 0.002 | 62.7 | |
| 0.2 | 0.016 | 125.3 | |
| 0.3 | 0.054 | 187.9 | |
| 0.4 | 0.127 | 250.5 | |
| 0.5 | 0.249 | 313.1 | |
| 0.7 | 0.683 | 438.2 | |
| 0.9 | 1.452 | 563.2 | |
| 1.0 | 1.992 | 625.7 | |
| 1.0 | 24.900 | 626.1 | |
| 30.0 | | | 10 |
| 0.0 | 0.000 | 0.0 | |
| 0.1 | 0.002 | 235.4 | |
| 0.2 | 0.016 | 470.5 | |
| 0.3 | 0.054 | 705.4 | |
| 0.4 | 0.127 | 940.3 | |
| 0.5 | 0.249 | 1175.1 | |
| 0.7 | 0.683 | 1644.5 | |
| 0.9 | 1.452 | 2113.9 | |
| 1.0 | 1.992 | 2348.5 | |
| 1.0 | 24.900 | 2350.1 | |
| 78.0 | | | 10 |

Figure 7.2. Example of p-y calculations using spreadsheet *PYPILE* (1 of 2).

| | | | | |
|-----------------------------|--------------|-----------|------------------|--|
| Depth (in) =====> | 78.0 | 10 | <===== | No. of data points defining p-y curve |
| 0.0 | 0.000 | 0.0 | | |
| 0.1 | 0.005 | 188.2 | | |
| 0.2 | 0.040 | 376.0 | | |
| 0.3 | 0.134 | 563.8 | | |
| 0.4 | 0.319 | 751.6 | | |
| 0.5 | 0.623 | 939.3 | | |
| 0.7 | 1.708 | 1314.5 | | |
| 0.9 | 3.630 | 1689.7 | | |
| 1.0 | 4.980 | 1877.2 | | |
| 1.0 | 62.250 | 1878.5 | | |
| Depth (in) =====> | 174.0 | 10 | <===== | No. of data points defining p-y curve |
| 0.0 | 0.000 | 0.0 | | |
| 0.1 | 0.004 | 142.2 | | |
| 0.2 | 0.032 | 284.2 | | |
| 0.3 | 0.108 | 426.1 | | |
| 0.4 | 0.255 | 568.0 | | |
| 0.5 | 0.498 | 709.8 | | |
| 0.7 | 1.367 | 993.4 | | |
| 0.9 | 2.904 | 1276.9 | | |
| 1.0 | 3.984 | 1418.7 | | |
| 1.0 | 49.800 | 1419.6 | | |
| Depth (in) =====> | 186.0 | 10 | <===== | No. of data points defining p-y curve |
| 0.0 | 0.000 | 0.0 | | |
| 0.1 | 0.000 | 331.6 | | |
| 0.2 | 0.003 | 662.8 | | |
| 0.3 | 0.011 | 993.8 | | |
| 0.4 | 0.025 | 1324.6 | | |
| 0.5 | 0.050 | 1655.4 | | |
| 0.7 | 0.137 | 2316.8 | | |
| 0.9 | 0.290 | 2978.0 | | |
| 1.0 | 0.398 | 3308.5 | | |
| 1.0 | 4.980 | 3310.8 | | |
| Depth (in) =====> | 198.0 | 10 | <===== | No. of data points defining p-y curve |
| 0.0 | 0.000 | 0.0 | | |
| 0.1 | 0.004 | 365.4 | | |
| 0.2 | 0.032 | 730.2 | | |
| 0.3 | 0.108 | 1094.9 | | |
| 0.4 | 0.255 | 1459.4 | | |
| 0.5 | 0.498 | 1823.9 | | |
| 0.7 | 1.367 | 2552.6 | | |
| 0.9 | 2.904 | 3281.1 | | |
| 1.0 | 3.984 | 3645.3 | | |
| 1.0 | 49.800 | 3647.8 | | |

Figure 7.2-Continued. Example of p-y calculations using spreadsheet *PYPILE* (2 of 2).

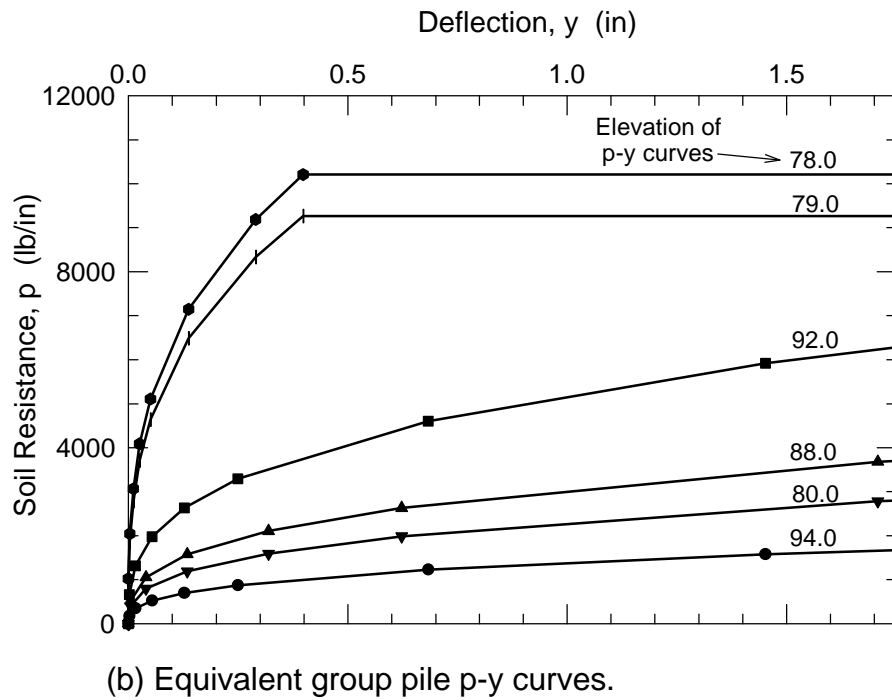
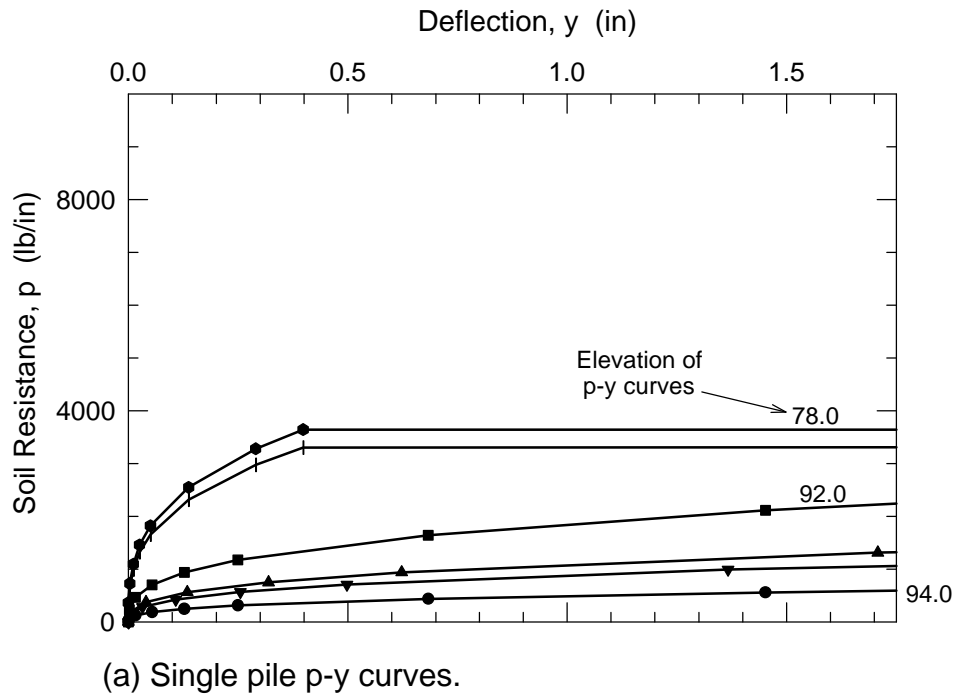


Figure 7.3. p-y curves for LPILE Plus 3.0 analyses.

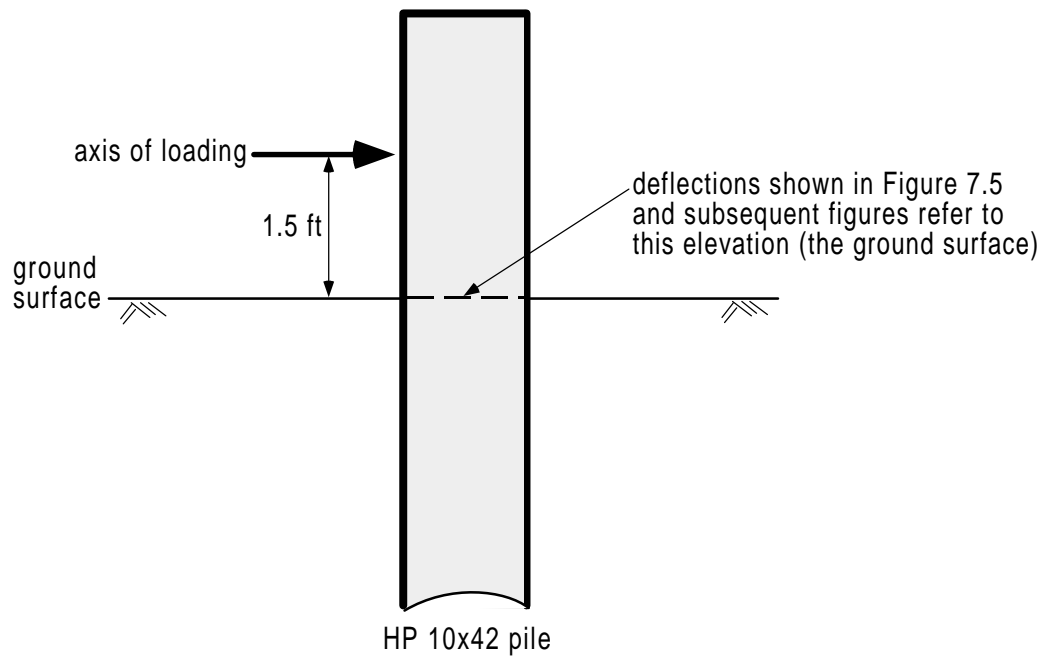
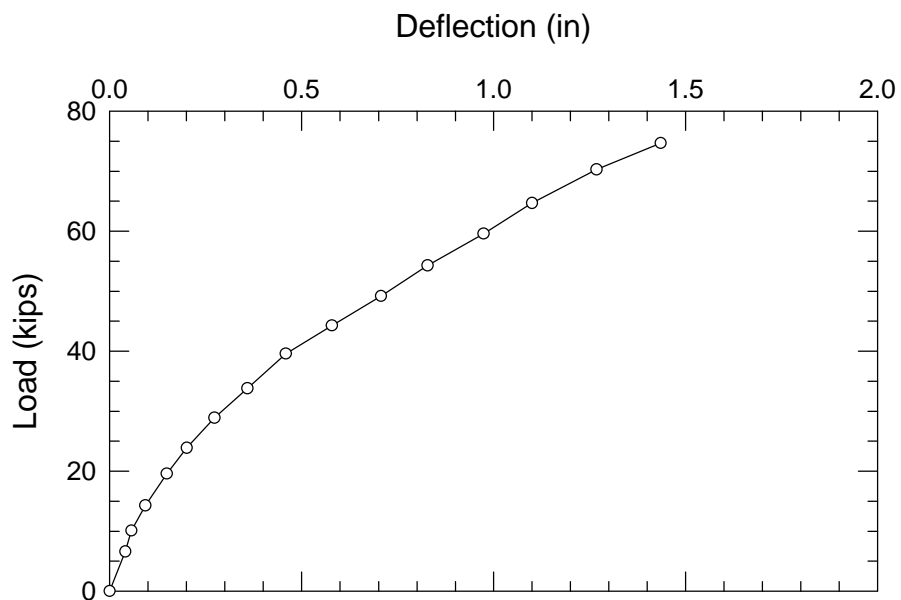
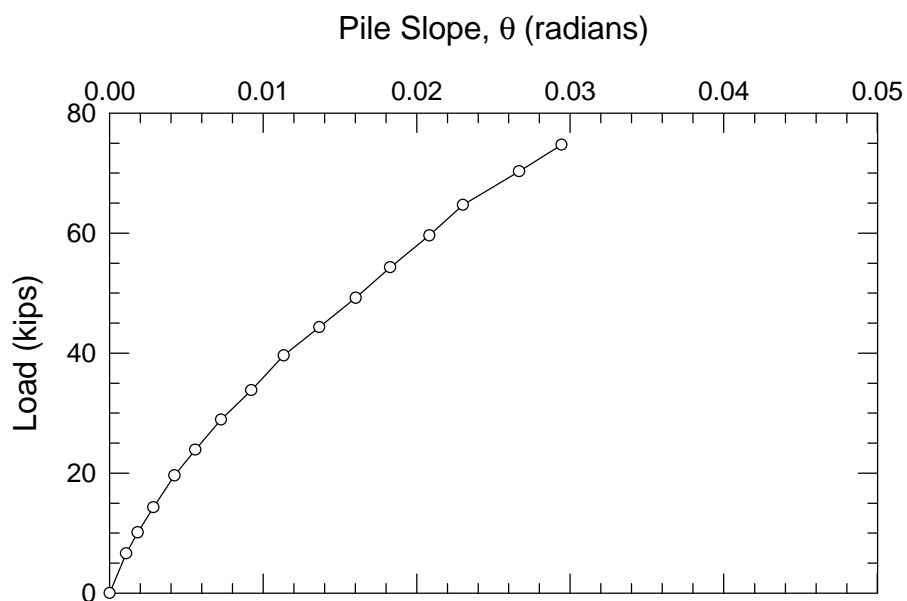


Figure 7.4. Single pile load testing arrangement.



(a) Measured load versus deflection response.



(b) Measured load versus pile-head rotation.

Figure 7.5. Measured response of south pile in natural soil.

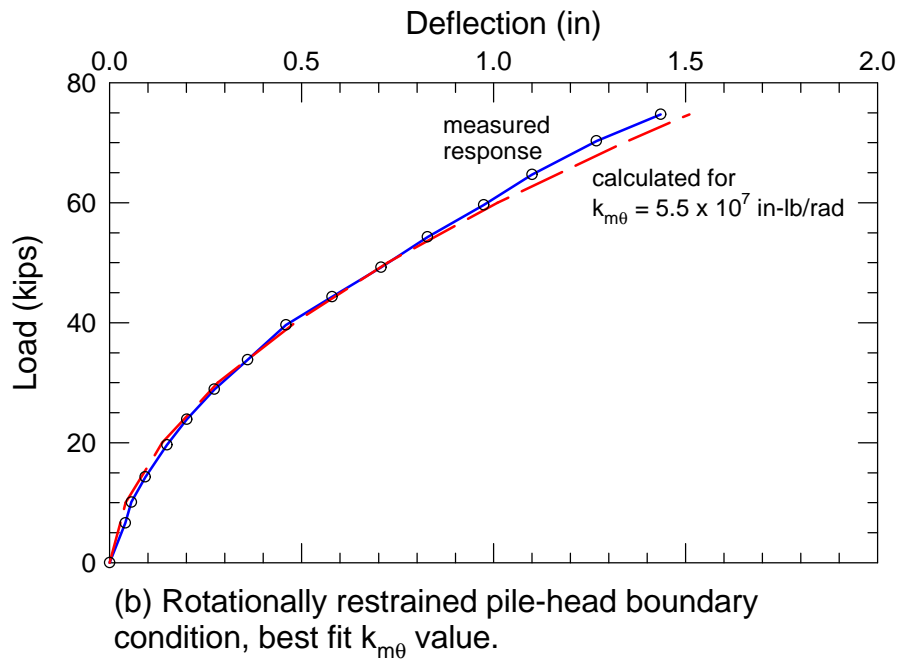
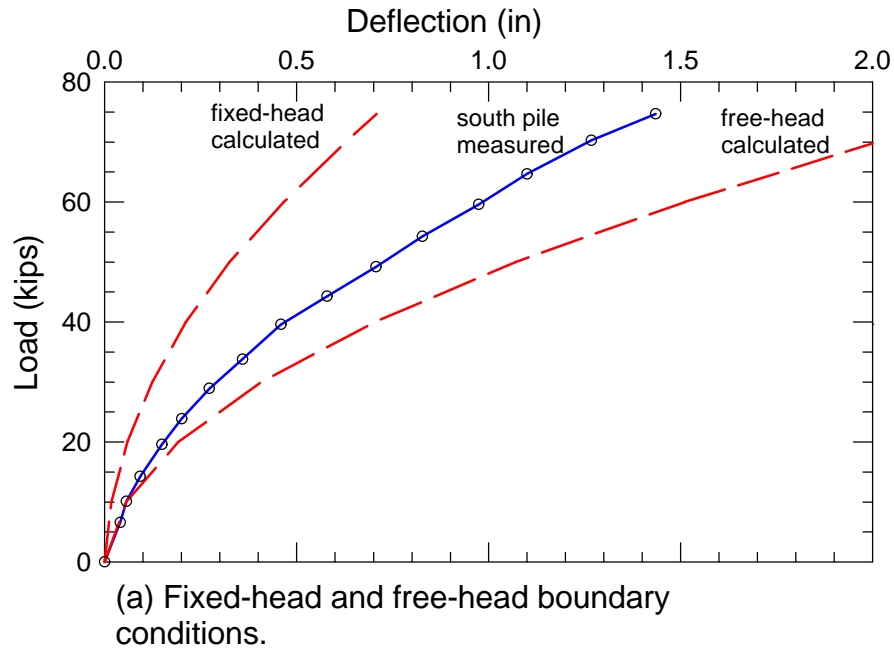


Figure 7.6. Calculated load-deflection curves for the south pile in natural soil, using p-y curves from *PYSHEET*.

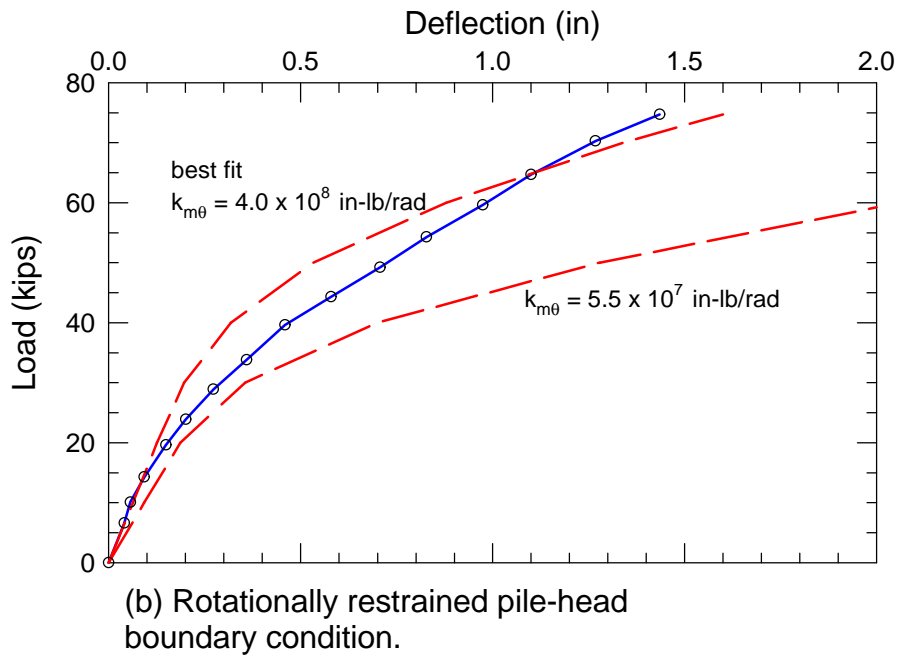
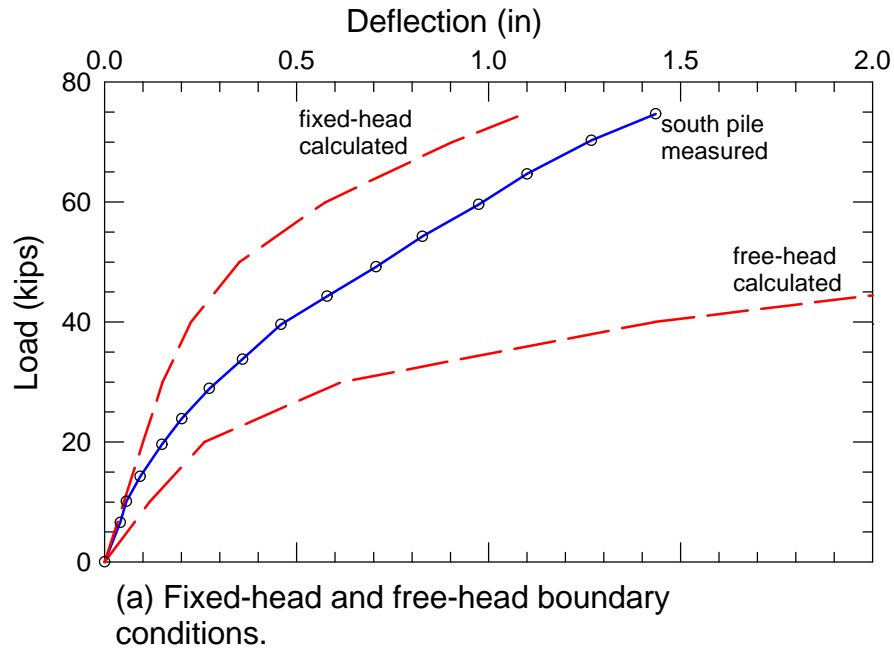
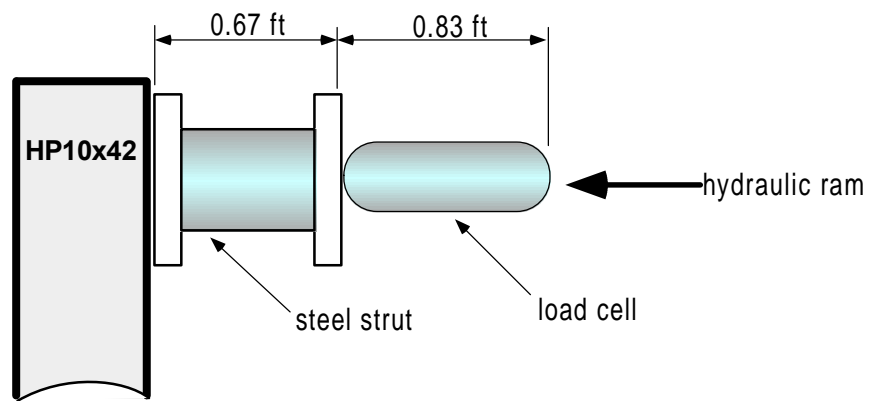
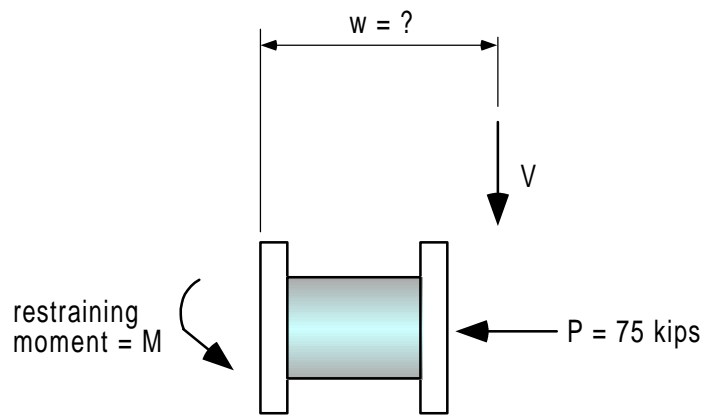


Figure 7.7. Calculated load-deflection curves for the south pile in natural soil, using *LPILE Plus 3.0* default p-y curves.

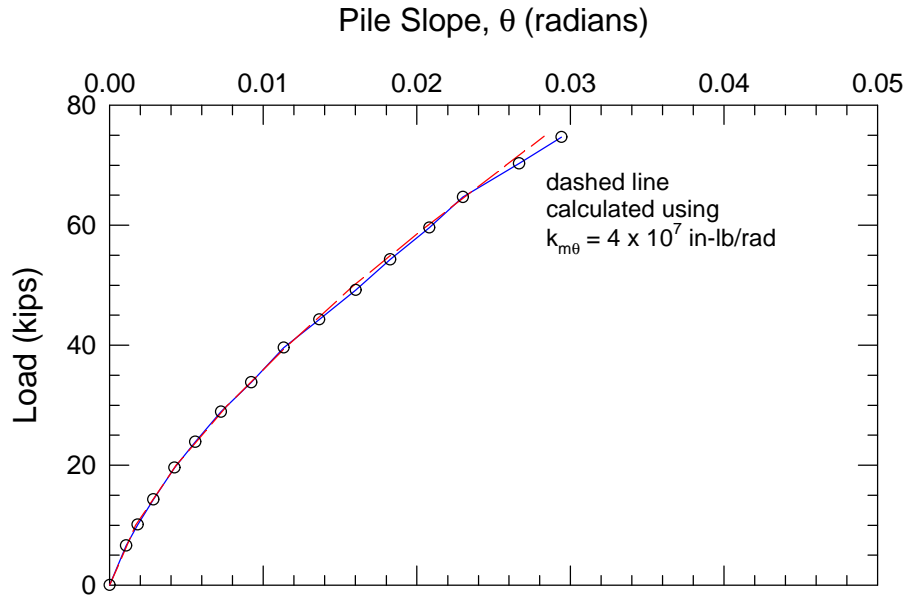


(a) Conceptual diagram of load connections.

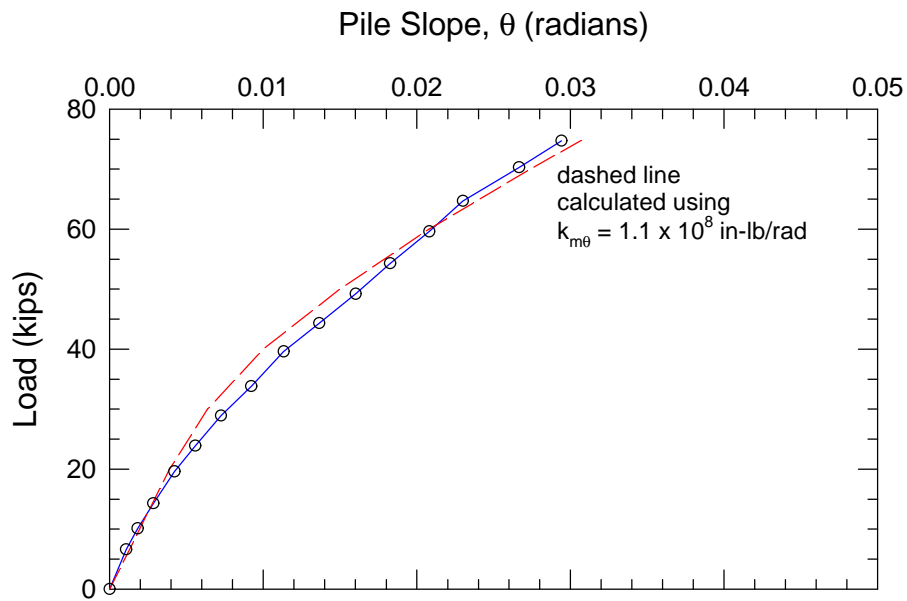


(b) Free-body-diagram of rigid strut connection.

Figure 7.8. Pile-head loading connection.



(a) Calculated response using Mokwa et al. (1997) p-y curves from *PYSHEET*.



(b) Calculated response using Reese (1997) "default" p-y curves from *LPILE Plus 3.0*.

Figure 7.9. Calculated slope versus deflection curves for the south pile using best match $k_{m\theta}$ values.

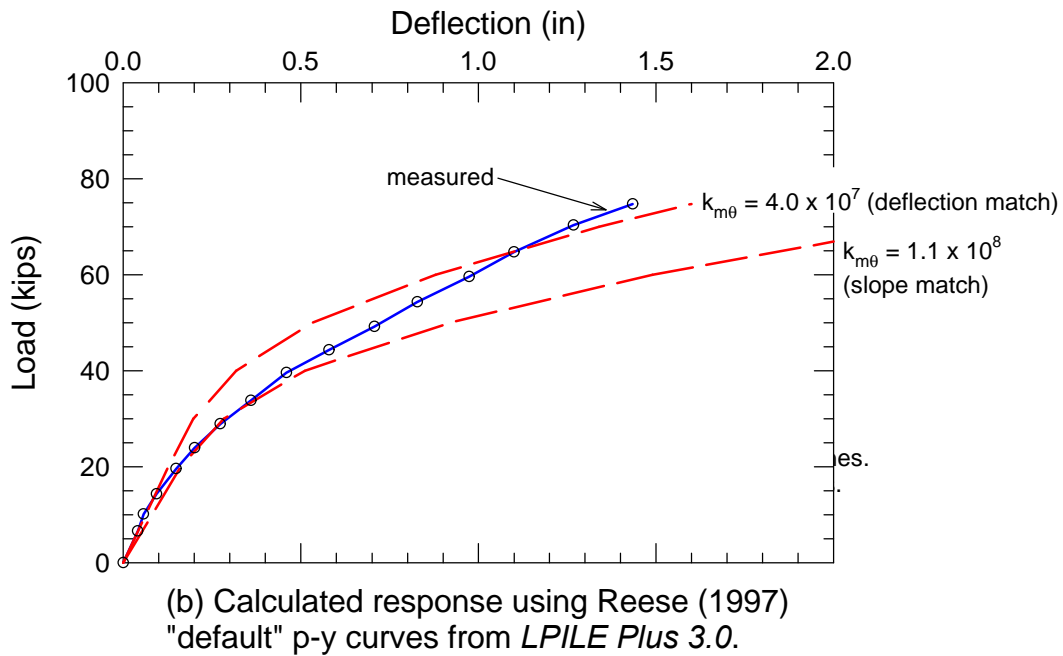
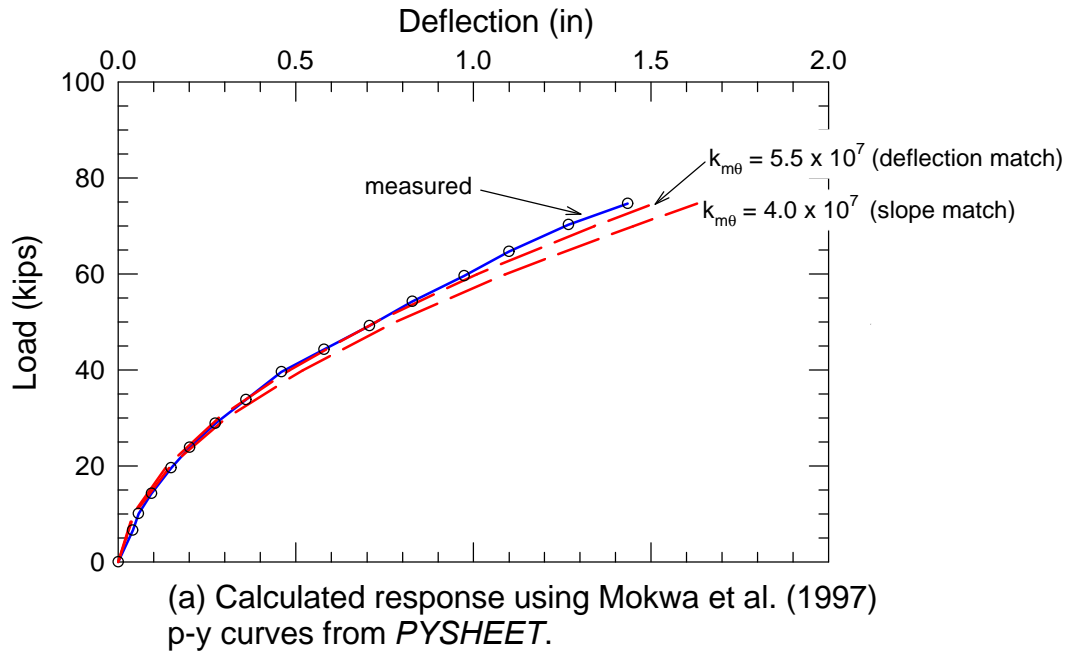
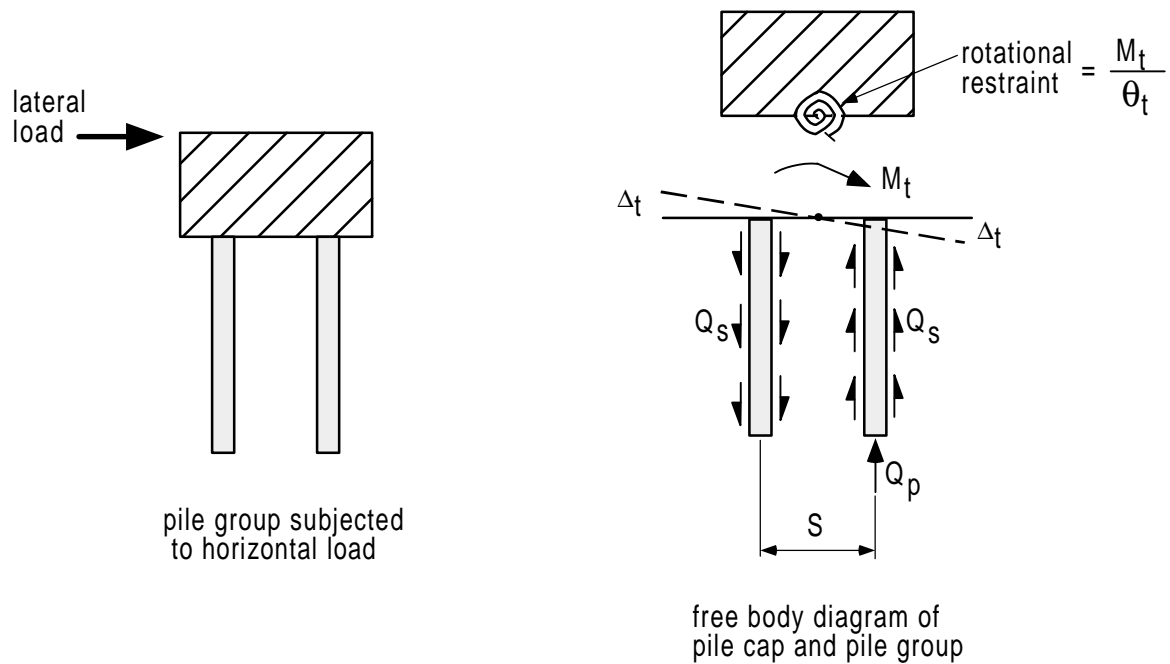
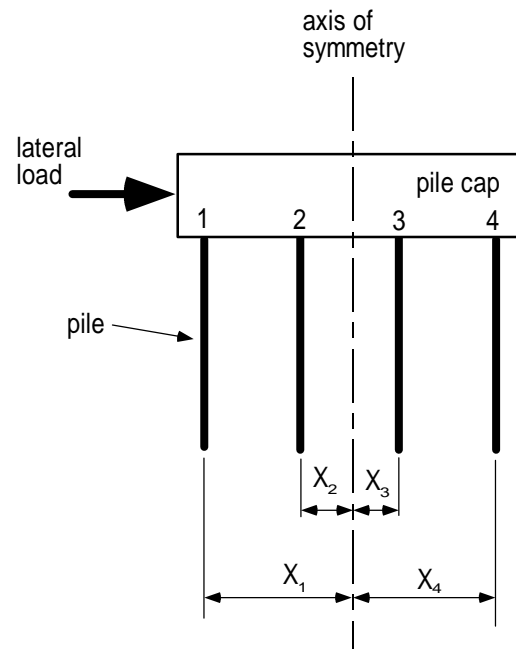


Figure 7.10. Comparison of calculated load versus deflection curves using best fit $k_{m\theta}$ ratios.

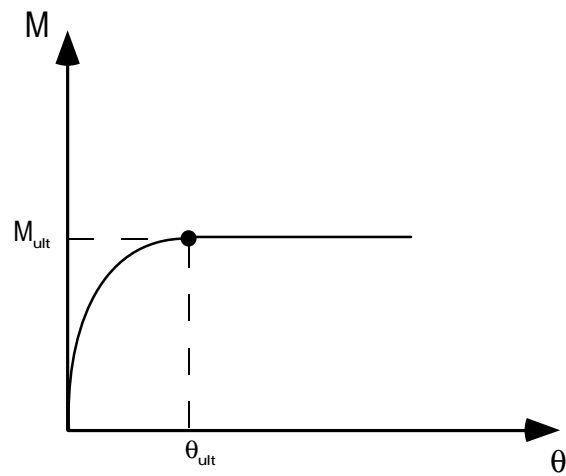


M_t = moment resisting rotation
 Δ_t = vertical displacement
 Q_s = pile side resistance force
 Q_p = pile end resistance force
 S = spacing between leading and trailing rows
 θ_t = angular rotation of cap and pile head

Figure 7.11. Conceptual model for estimating pile group rotational restraint.

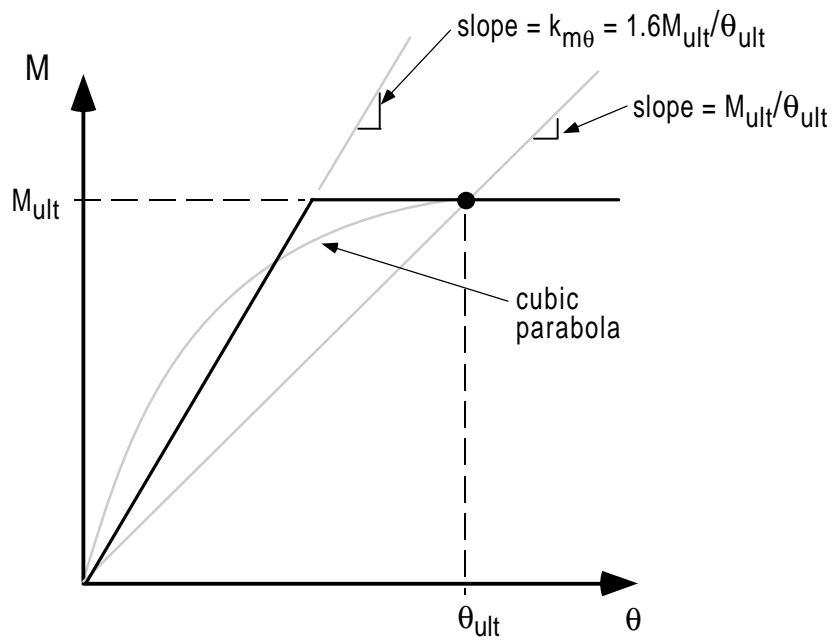


(a) Cross-section through a 4 by 4 pile group.

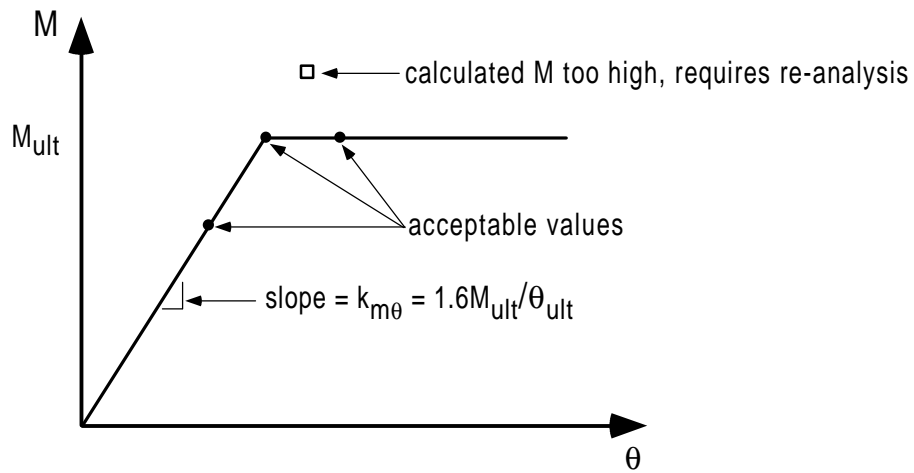


(b) Assumed relationship between M and θ .

Figure 7.12. Details for rotational restraint calculations.

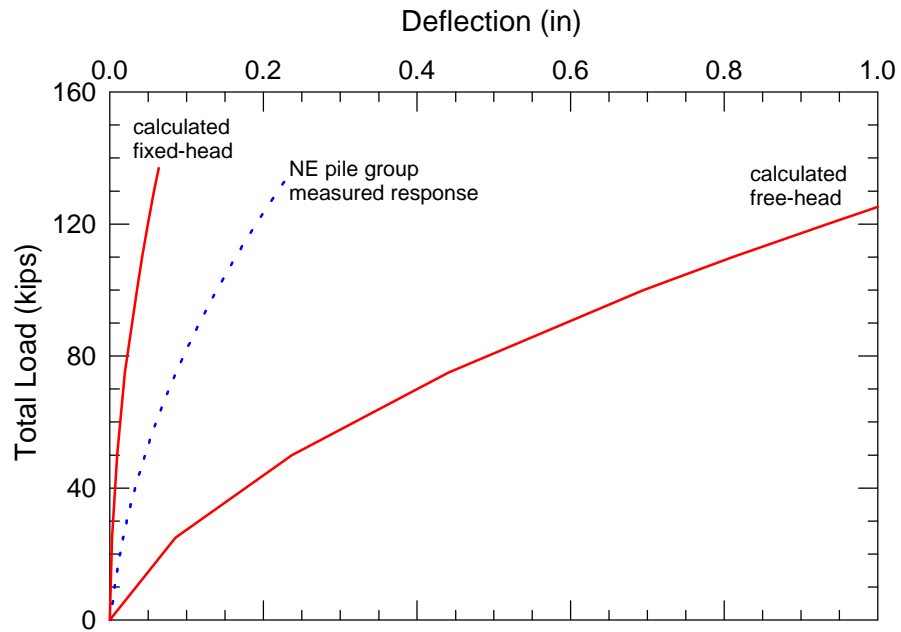


(a) Graphical illustration of $k_{m\theta}$ approximation.

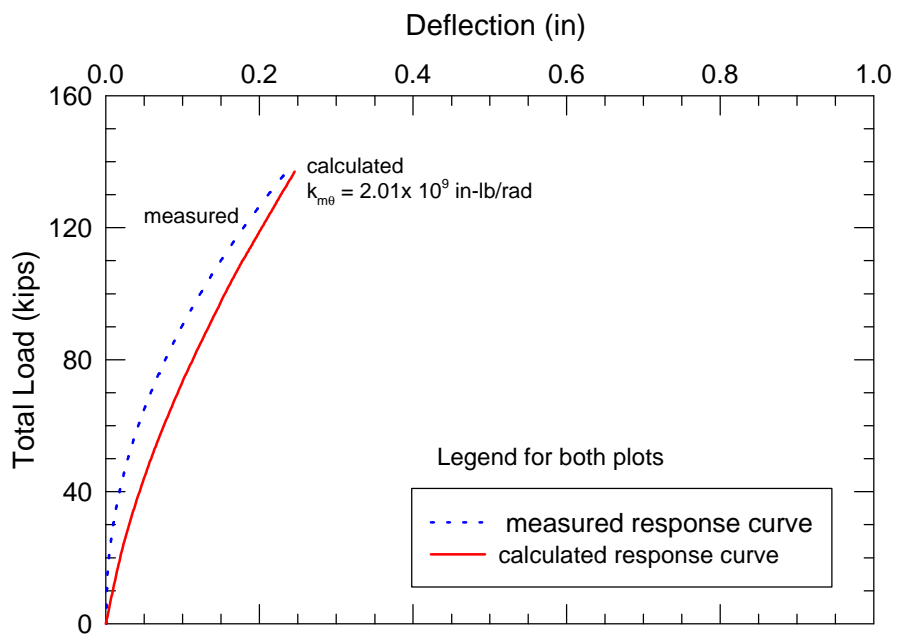


(b) Assumed $k_{m\theta}$ distribution for analysis and design

Figure 7.13. $k_{m\theta}$ approximation.



(a) Calculated response for fixed-head and free-head boundary conditions.



(b.) Calculated response for rotationally restrained pile head boundary condition.

Figure 7.14. Calculated response for the NE pile group with no cap resistance.

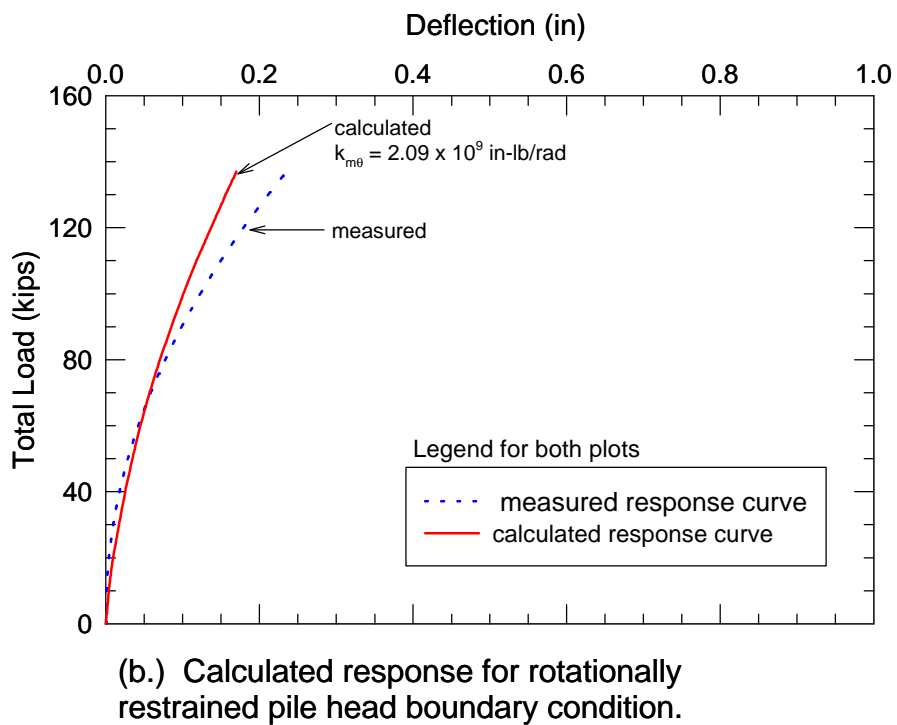
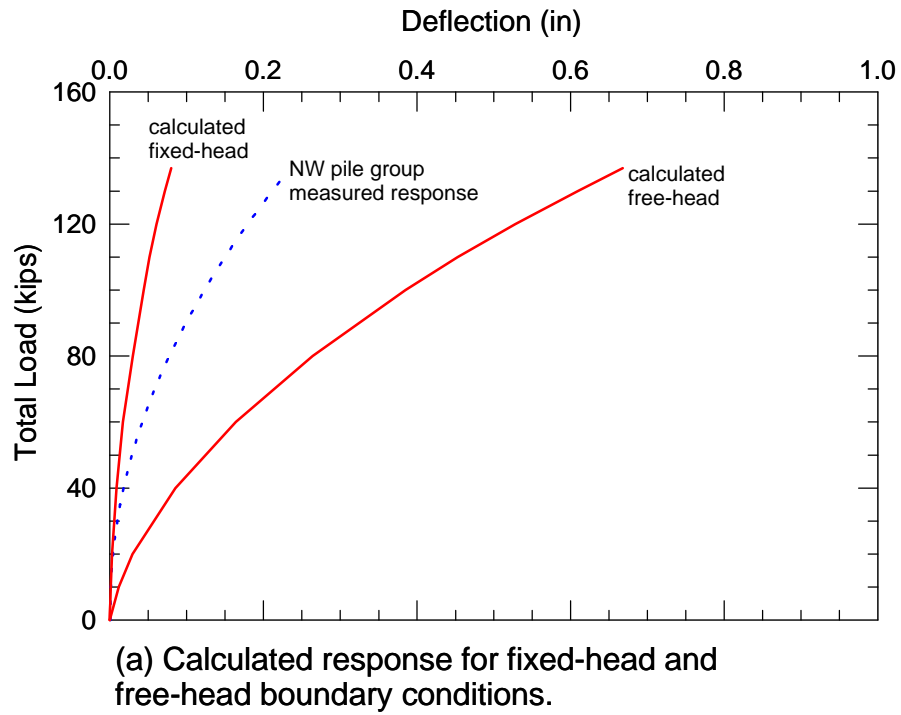


Figure 7.15. Calculated response for the NW pile group with no cap resistance.

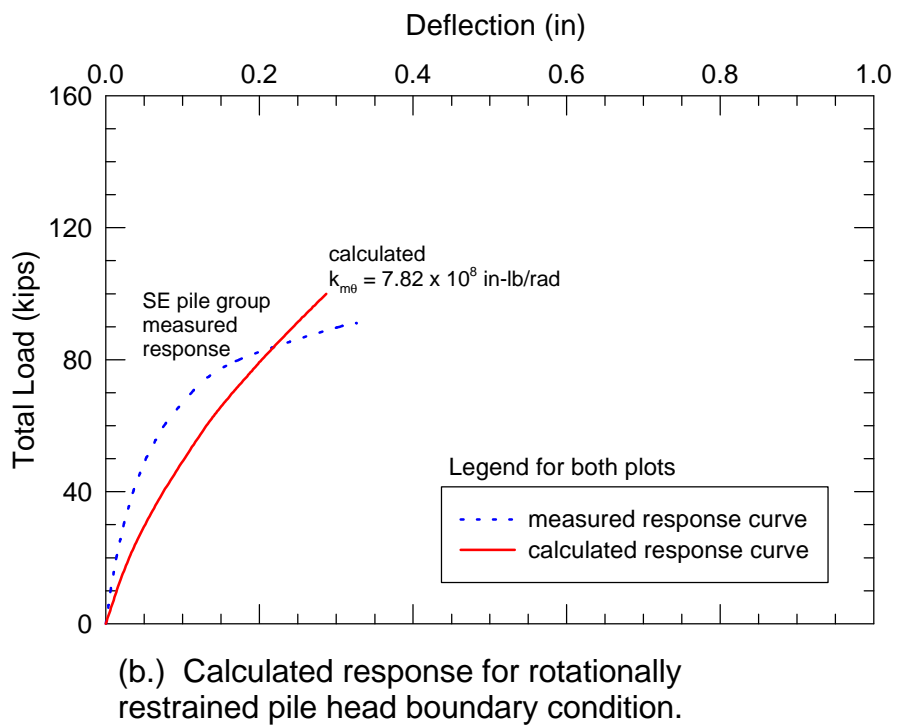
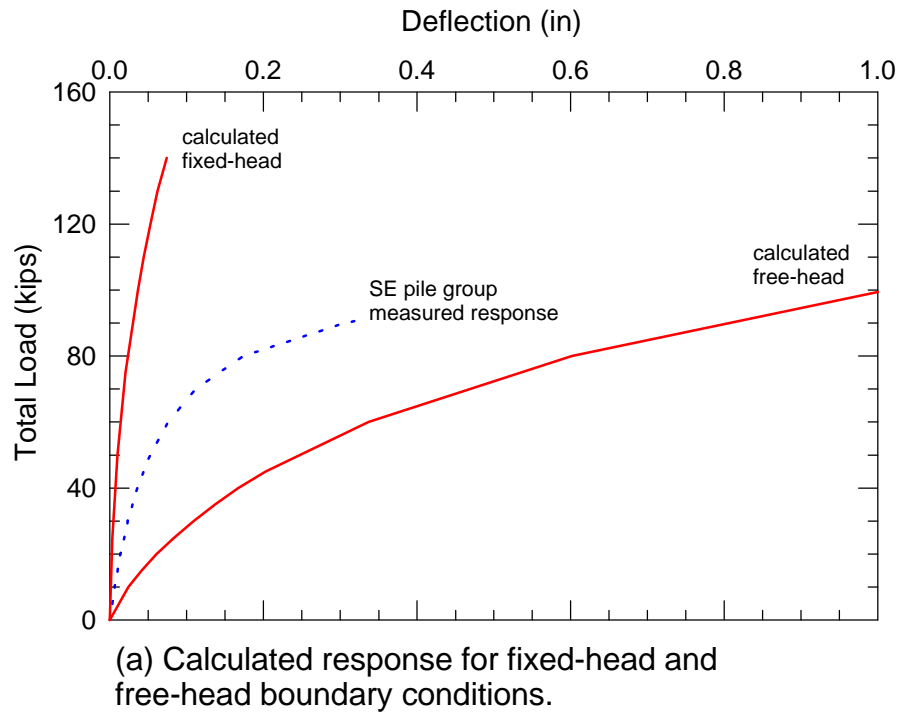
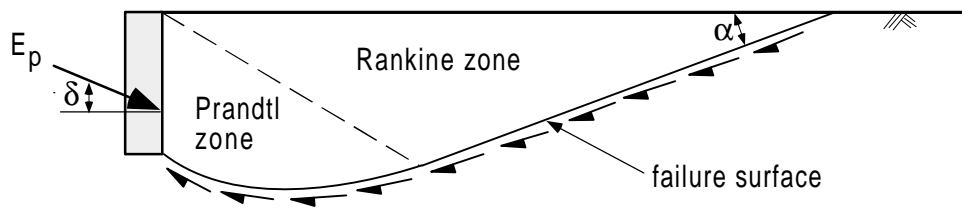


Figure 7.16. Calculated response for the SE pile group with no cap resistance.

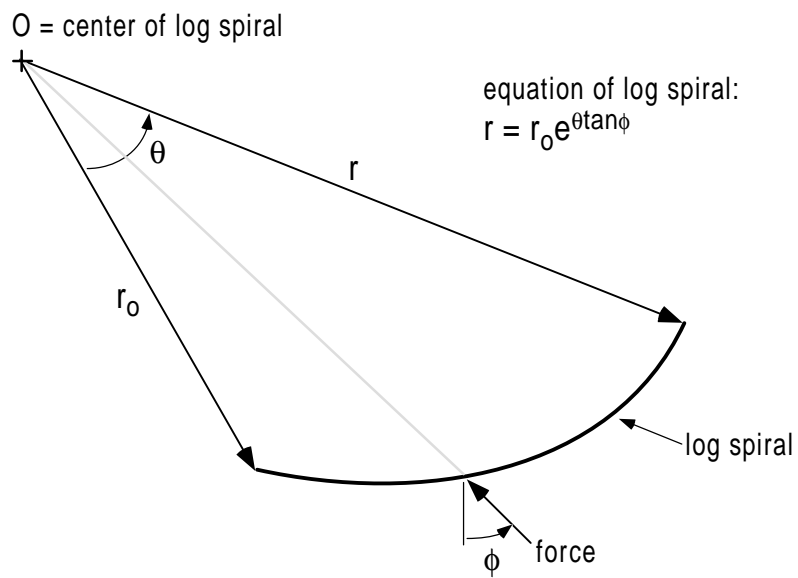


E_p = passive earth pressure

δ = wall friction angle

$\alpha = 45 - \phi/2$

(a) Theoretical shape of passive failure zone.



(b) Log spiral.

Figure 7.17. Log spiral approximation.

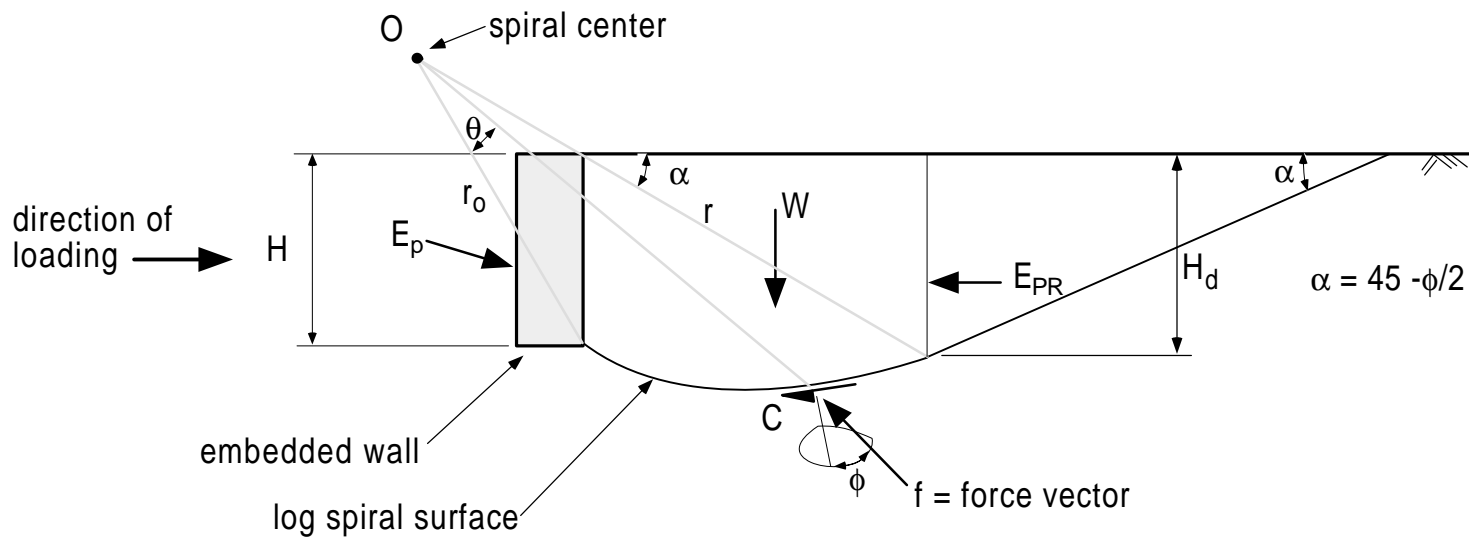
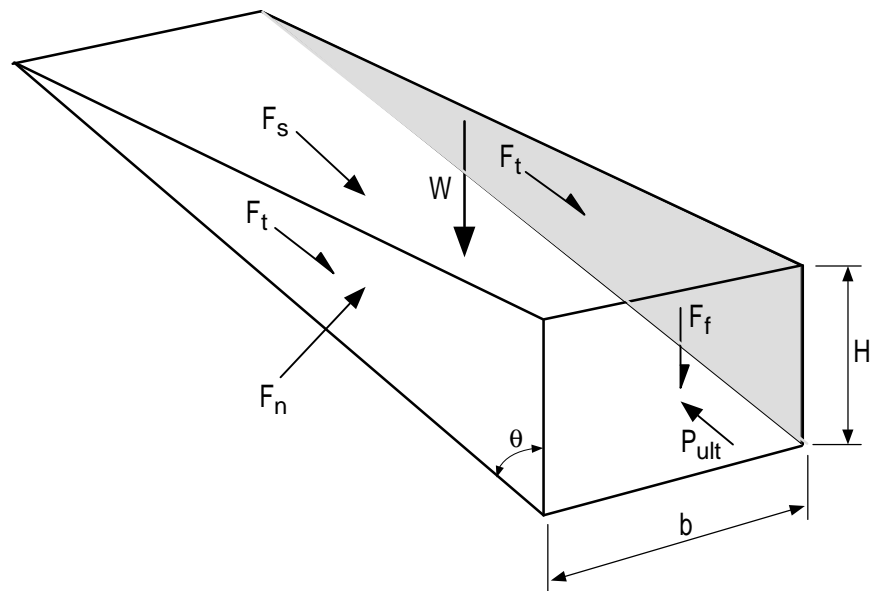
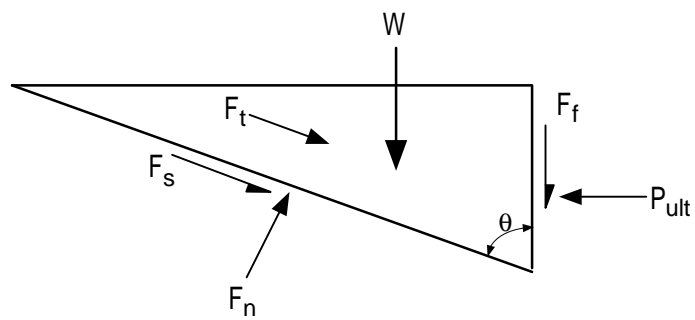


Figure 7.18. Graphical representation of the log spiral earth pressure method.

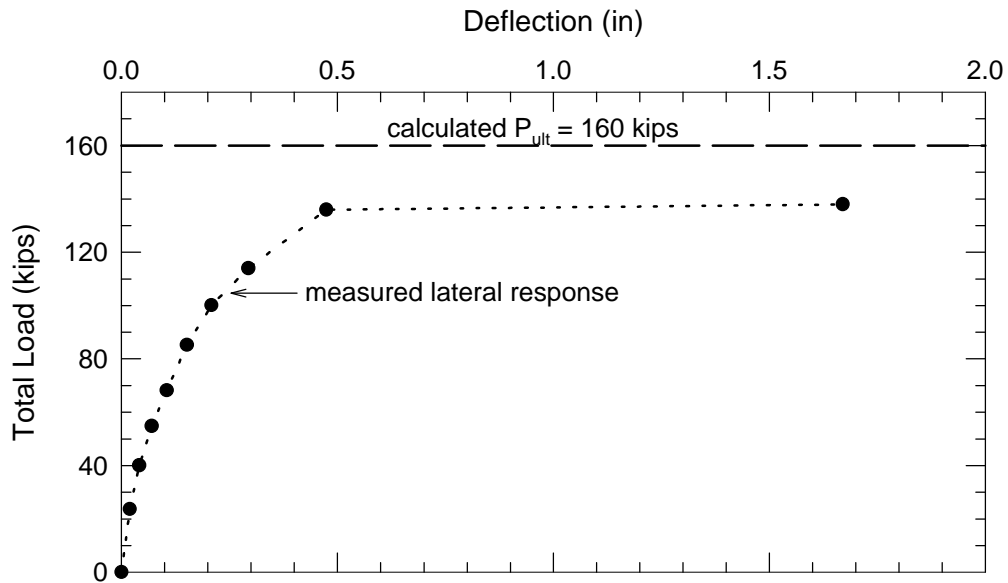


Orthogonal view of failure wedge

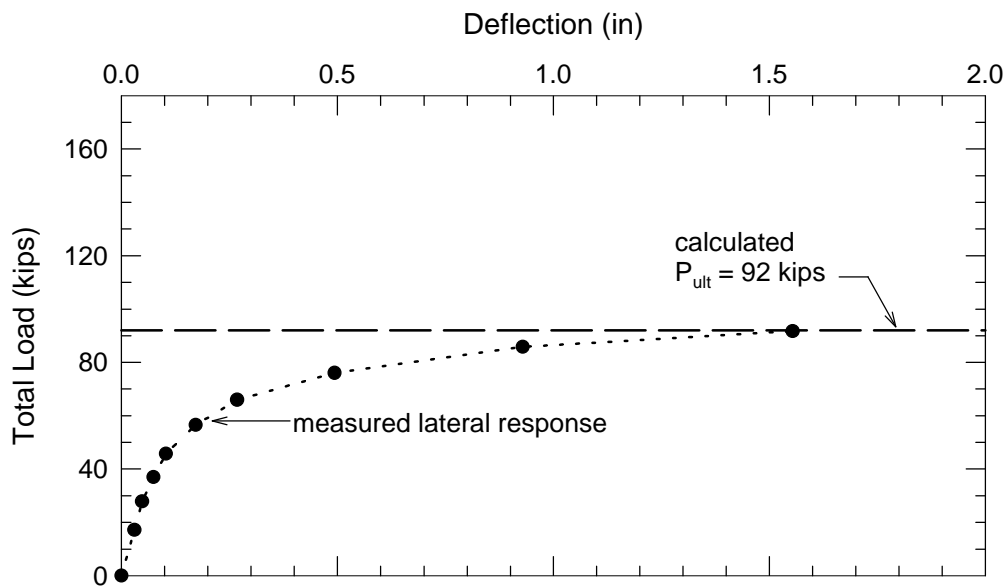


Side view of failure wedge

Figure 7.19. $\phi = 0$ passive wedge model.



(a) Bulkhead embedded in natural soil.



(b) Bulkhead backfilled with compacted crusher run gravel.

Figure 7.20. Comparison of measured and calculated passive resistance for bulkhead in natural soil and gravel.

Ultimate Capacity Calculation Sheet

Created by R.L. Mokwa and J.M. Duncan - August 1999

Date: 9/1/99
 Description: Bulkhead in natural soil
 Engineer: RLM

Input Values (red)

| | | |
|--|---|--------------|
| cap width, | b (ft) = | 6.30 |
| cap height, | H (ft) = | 3.50 |
| embedment depth, | z (ft) = | 0.00 |
| surcharge, | q _s (psf) = | 0.0 |
| cohesion, | c (psf) = | 970.0 |
| soil friction angle, | φ (deg.) = | 37.0 |
| wall friction, | δ (deg.) = | 3.5 |
| initial soil modulus, | E _i (kip/ft ²) = | 890 |
| poisson's ratio, | ν = | 0.33 |
| soil unit weight, | γ _m (pcf) = | 122.0 |
| adhesion factor, | α = | 0.00 |
| Δ _{max} /H, (0.04 suggested, see notes) = | | 0.04 |
| Calculated Values (blue) | | |
| K _a (Rankine) = | | 0.25 |
| K _p (Rankine) = | | 4.02 |
| K _p (Coulomb) = | | 4.56 |
| K _{pφ} (Log Spiral, soil weight) = | | 4.65 |
| K _{pq} (Log Spiral, surcharge) = | | 0.00 |
| K _{pc} (Log Spiral, cohesion) = | | 2.11 |
| E _p (kip/ft) = | | 17.81 |
| Ovesen's 3-D factor, R = | | 1.43 |
| k _{max} , elastic stiffness (kip/in) = | | 890.5 |
| P_{ult} (kips) = | | 160.4 |

Figure 7.21. *PYCAP Summary* worksheet for bulkhead in natural soil.

Ultimate Capacity Calculation Sheet

Created by R.L. Mokwa and J.M. Duncan - August 1999

Date: 9/1/99
 Description: Bulkhead backfilled with compacted gravel
 Engineer: RLM

Input Values (red)

| | | |
|--|--------------------------------|--------------|
| cap width, | b (ft) = | 6.30 |
| cap height, | H (ft) = | 3.50 |
| embedment depth, | z (ft) = | 0.00 |
| surcharge, | q_s (psf) = | 0.0 |
| cohesion, | c (psf) = | 0.0 |
| soil friction angle, | ϕ (deg.) = | 50.0 |
| wall friction, | δ (deg.) = | 6.2 |
| initial soil modulus, | E_i (kip/ft ²) = | 760 |
| poisson's ratio, | ν = | 0.3 |
| soil unit weight, | γ_m (pcf) = | 134.0 |
| adhesion factor, | α = | 0.00 |
| Δ_{max}/H , (0.04 suggested, see notes) = | | 0.04 |
| Calculated Values (blue) | | |
| K_a (Rankine) = | | 0.13 |
| K_p (Rankine) = | | 7.55 |
| K_p (Coulomb) = | | 10.41 |
| $K_{p\phi}$ (Log Spiral, soil weight) = | | 10.22 |
| K_{pq} (Log Spiral, surcharge) = | | 0.00 |
| K_{pc} (Log Spiral, cohesion) = | | 0.00 |
| E_p (kip/ft) = | | 8.39 |
| Ovesen's 3-D factor, R = | | 1.75 |
| k_{max} , elastic stiffness (kip/in) = | | 756.4 |
| P_{ult} (kips) = | | 92.3 |

Figure 7.22. *PYCAP Summary* worksheet for bulkhead backfilled with compacted gravel.

Elasticity Solution for Horizontal Loading on a Vertical Rectangle

Created by R.L. Mokwa - August 1999

Reference: Douglas, D.J. and Davis, E.H. (1964). *Geotechnique*, Vol.14(3), p. 115-132.

Description: Bulkhead in natural soil

Date: 9/1/99

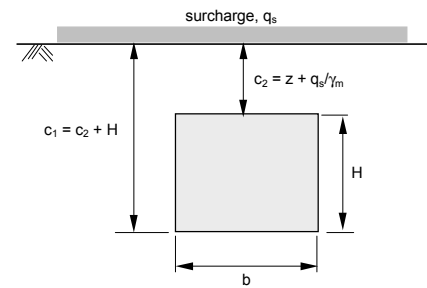
Equations

$$y_1 = \frac{P(1+\nu)(I_1)}{16\pi H E_i(1-\nu)} \quad y_2 = \frac{P(1+\nu)(I_2)}{16\pi H E_i(1-\nu)}$$

Input Parameters

y_1 = horizontal deflection at upper corner of rectangle
 y_2 = horizontal deflection at lower corner of rectangle
 P = applied force
 ν = Poisson's ratio
 E_i = Initial tangent soil modulus
 H = rectangle height
 F_1, F_4, F_5 = influence factors
 c_1, c_2, d = dimensions defined in diagram
 $I_1 = \{ (3-4\nu)F_1 + F_4 + 4(1-2\nu)(1-\nu)F_5 \}$
 $I_2 = \{ (3-4\nu)F_1 + F_2 + 4(1-2\nu)(1-\nu)F_3 \}$

$y_{avg} = (y_1 + y_2)/2$
 k_{max} = Initial elastic stiffness
 = slope of P versus y_{avg} line
 $k_{max} = P/y_{avg}$



Input from Summary Sheet

$\nu = 0.33$
 $E_i \text{ (kip/ft}^2\text{)} = 890$
 $h \text{ (ft)} = 3.50$
 $b \text{ (ft)} = 6.30$
 $c_1 \text{ (ft)} = 3.50$
 $c_2 \text{ (ft)} = 0.00$

Calculated Values

$K_1 = 2c_1/b = 1.111$
 $K_2 = 2c_2/b = 0.000$
 $F_1 = 2.561$
 $F_2 = 1.474$
 $F_3 = 0.625$
 $F_4 = 2.561$
 $F_5 = 1.703$
 $I_1 = 8.416$
 $I_2 = 6.346$

Results

Initial elastic stiffness, k_{max}

$k_{max} = 890.5$ kips/inch

Figure 7.23. *Elasticity* worksheet for the bulkhead in natural soil.

Hyperbolic Calculation Sheet

Created by R.L. Mokwa - August 1999

Description: Bulkhead in natural soil

Hyperbolic equation: $P = y / \{ (1/k_{\max}) + (yR_f/P_{ult}) \}$ $R_f = \{ (\Delta_{\max}/P_{ult}) - (1/k) \} (P_{ult}/\Delta_{\max})$

Input values - Use "Summary" worksheet for data entry.

k_{\max} (kips/in) = 890.5
H (ft) = 3.50
 P_{ult} = 160.4

Δ_{\max}/H = 0.04
 Δ_{\max} (in) = 1.68
 R_f = 0.89

Calculated values using hyperbolic formulation

| Def. (in) | Load (kips) |
|-----------|-------------|
| y | P |
| 0 | 0.00 |
| 0.01 | 8.48 |
| 0.03 | 23.26 |
| 0.05 | 35.68 |
| 0.1 | 59.54 |
| 0.15 | 76.62 |
| 0.2 | 89.45 |
| 0.25 | 99.43 |
| 0.3 | 107.43 |
| 0.35 | 113.98 |
| 0.4 | 119.44 |
| 0.45 | 124.06 |
| 0.5 | 128.02 |
| 0.55 | 131.46 |
| 0.6 | 134.46 |
| 0.65 | 137.12 |
| 0.7 | 139.48 |
| 0.75 | 141.59 |
| 0.8 | 143.49 |
| 0.85 | 145.21 |
| 0.9 | 146.78 |
| 0.95 | 148.21 |
| 1 | 149.51 |
| 1.05 | 150.72 |
| 1.1 | 151.83 |
| 1.15 | 152.86 |
| 1.2 | 153.82 |
| 1.25 | 154.71 |
| 1.3 | 155.54 |
| 1.35 | 156.32 |
| 1.4 | 157.05 |
| 1.45 | 157.73 |
| 1.5 | 158.38 |
| 1.55 | 158.99 |
| 1.6 | 159.56 |
| 1.65 | 160.10 |
| 1.7 | 160.62 |
| 1.75 | 161.11 |
| 1.8 | 161.57 |
| 1.85 | 162.01 |

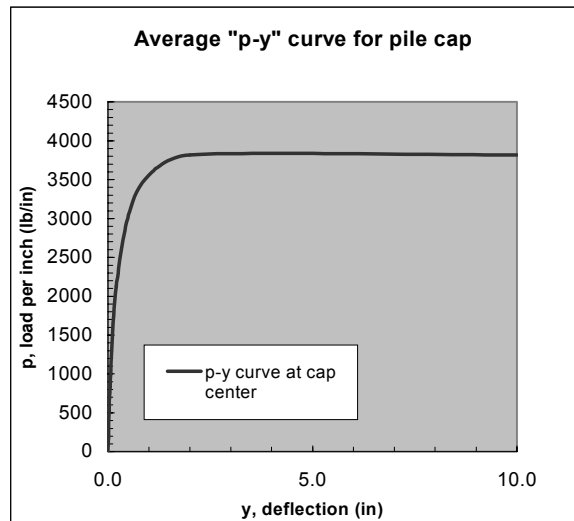
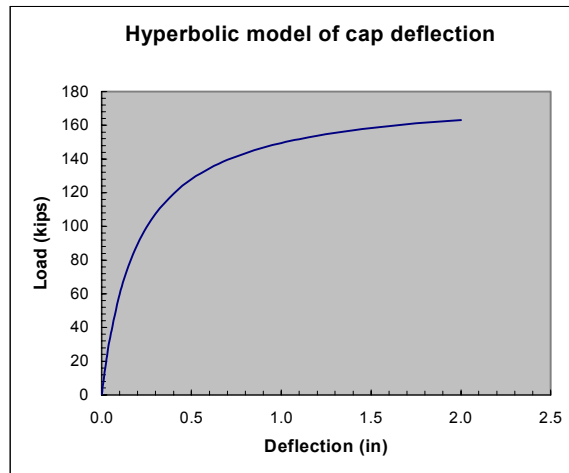
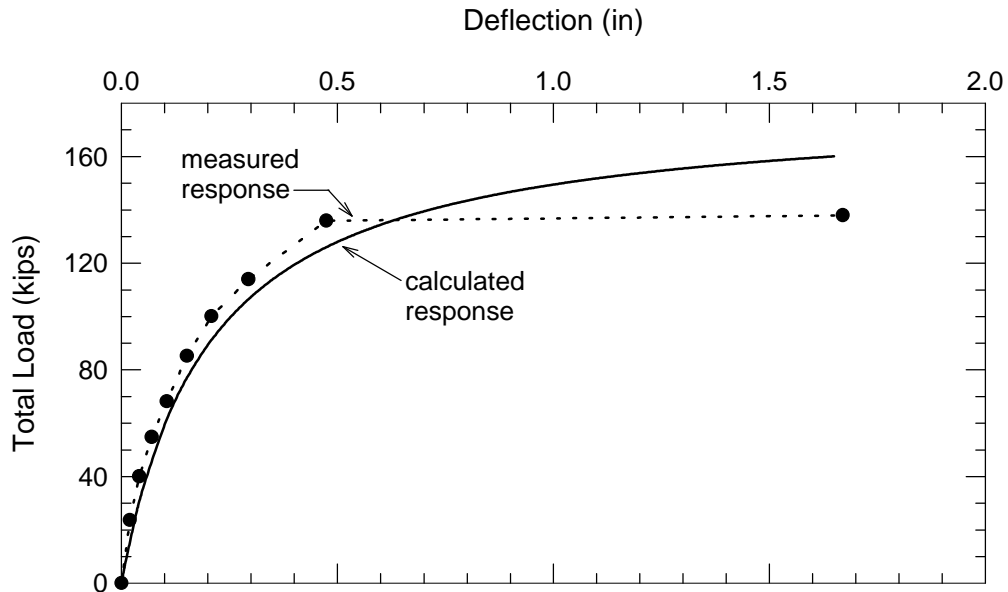
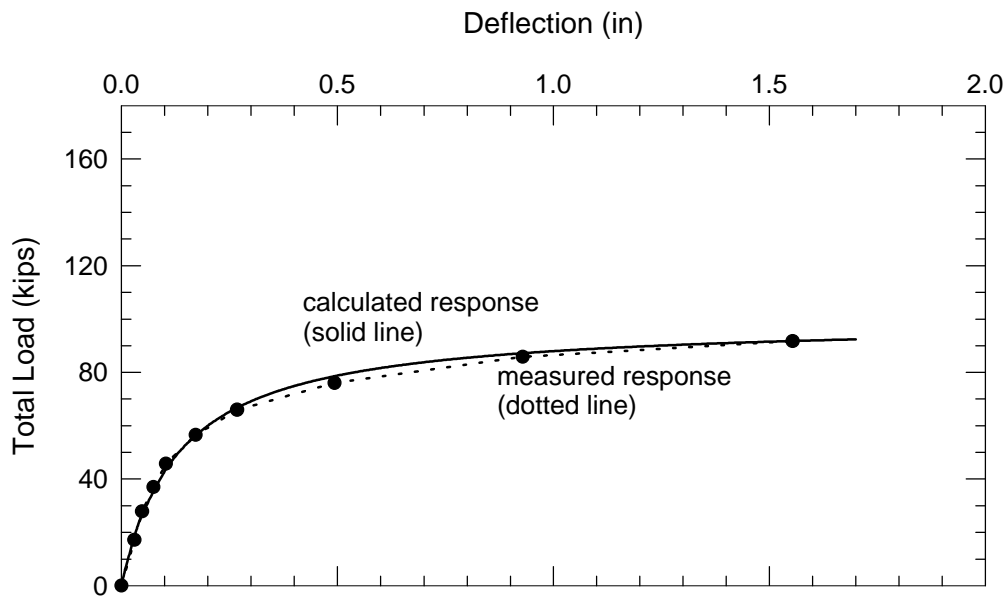


Figure 7.24. *Hyperbola* worksheet for the bulkhead in natural soil.



(a) Bulkhead embedded in natural soil.



(b) Bulkhead backfilled with compacted crusher run gravel.

Figure 7.25. Comparison of calculated versus observed load-deflection behavior of bulkhead in natural soil and gravel.

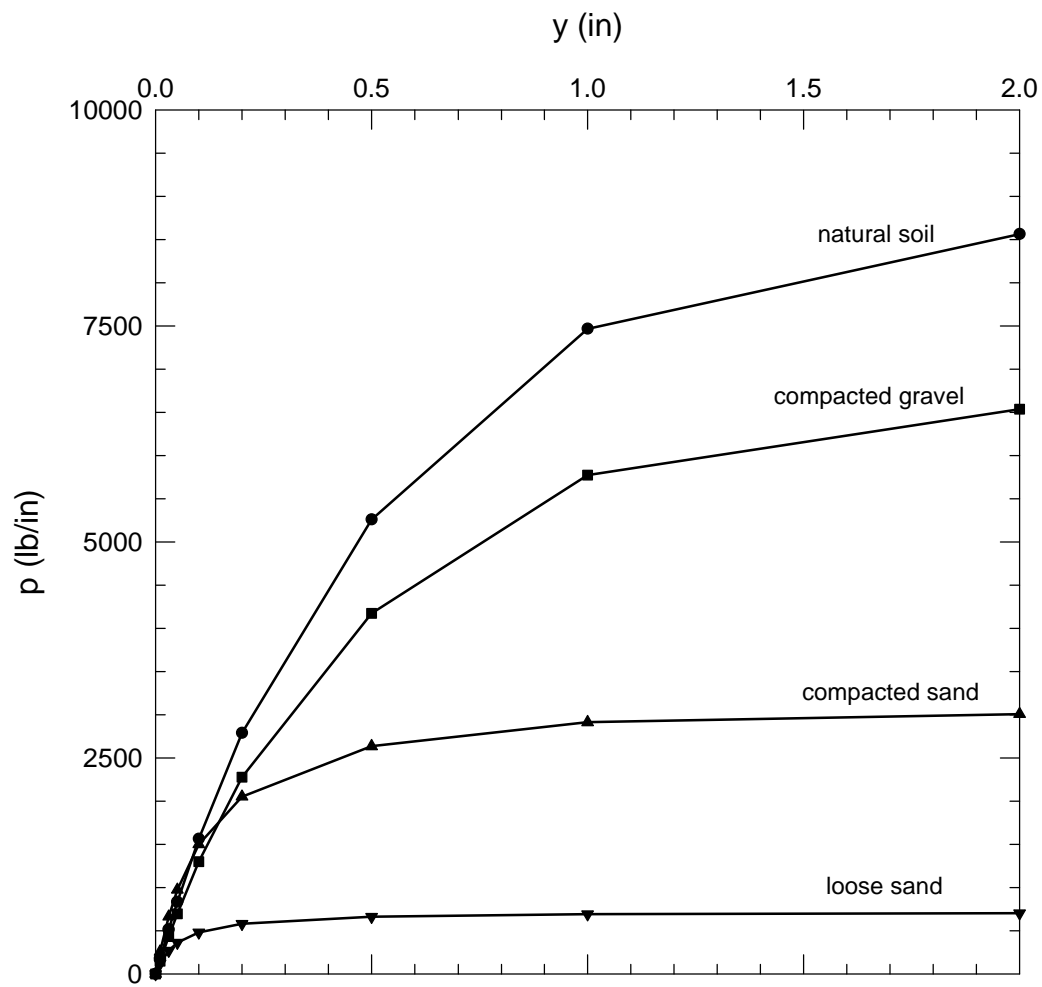


Figure 7.26. p - y curves for 36-in-deep pile cap in four different soils.

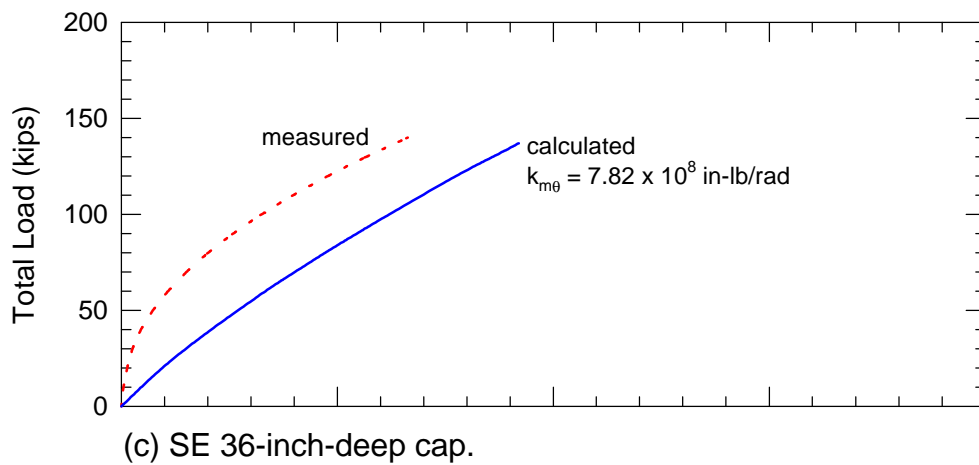
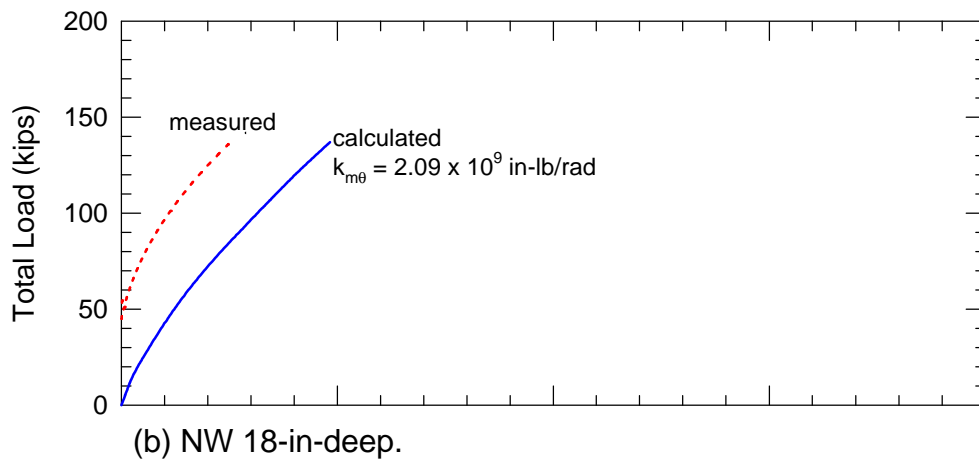
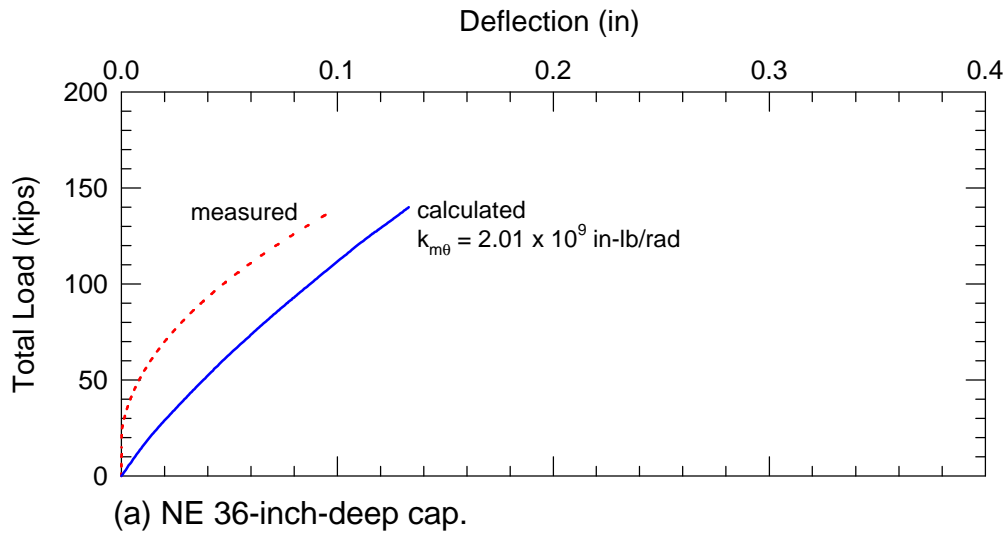
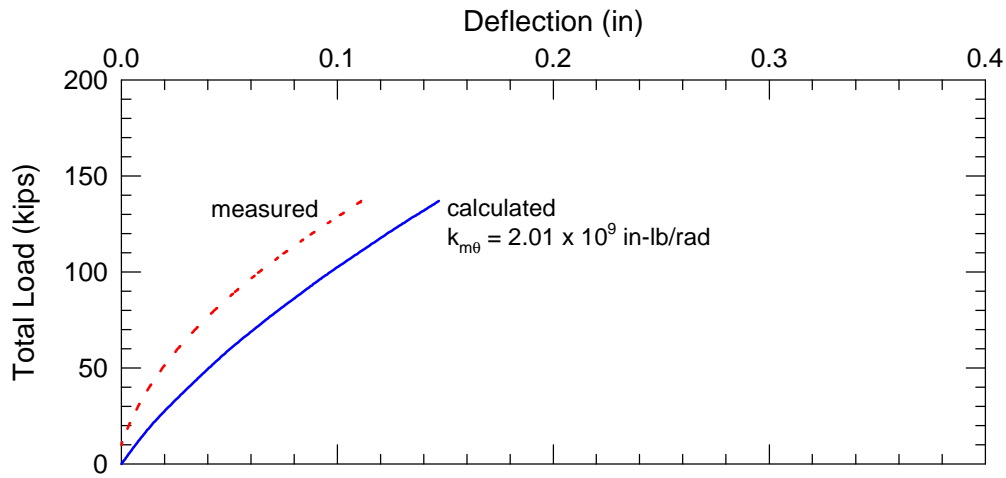
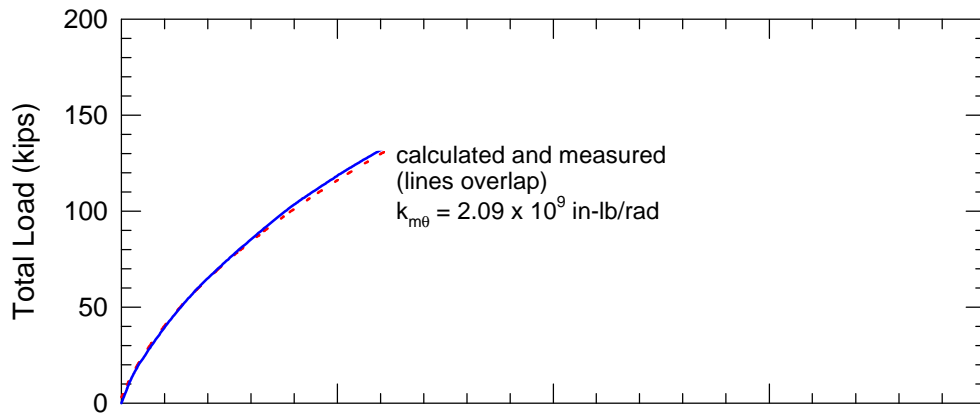


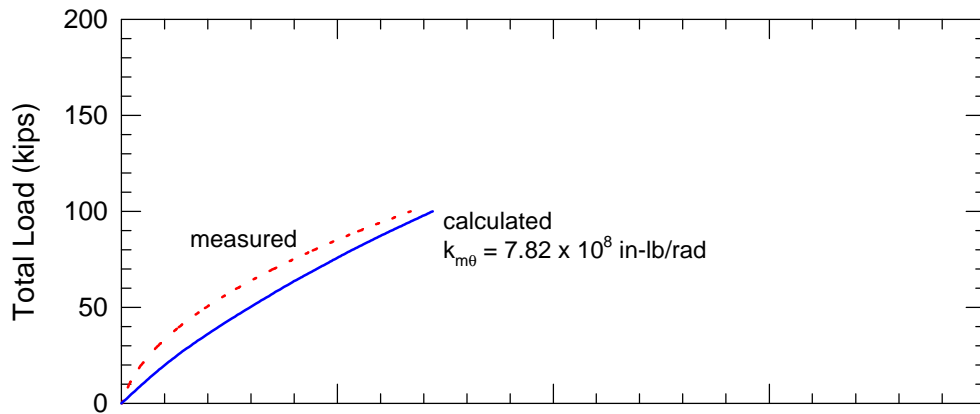
Figure 7.27. Comparison between calculated and measured responses for pile caps in natural soil.



(a) NE 36-inch-deep pile cap.



(b) NW 18-inch-deep cap.

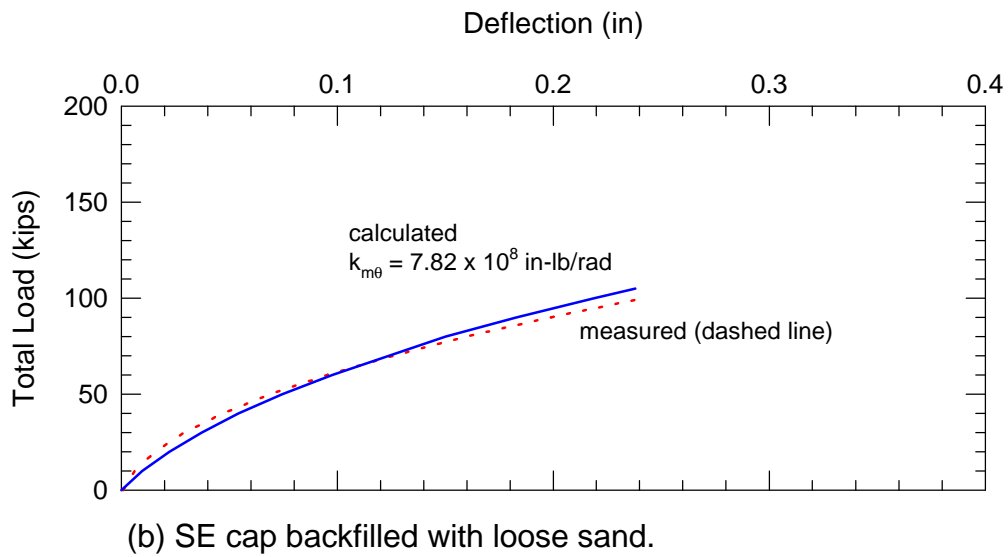
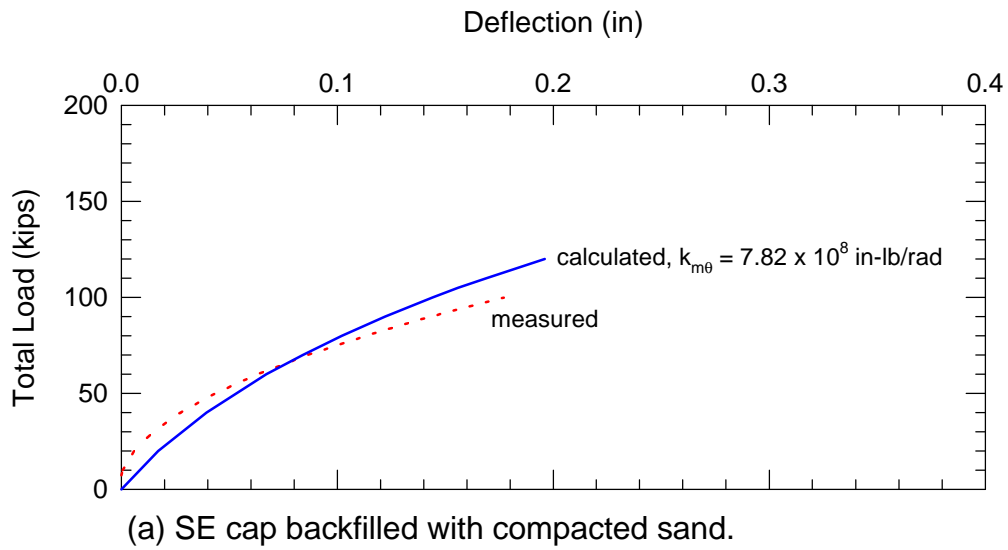


(c) SE 36-inch-deep cap.

Legend for all plots

--- measured response
— calculated response

Figure 7.28. Comparison between calculated and measured responses for pile caps backfilled with crusher run gravel.



Legend for both plots

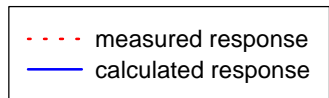
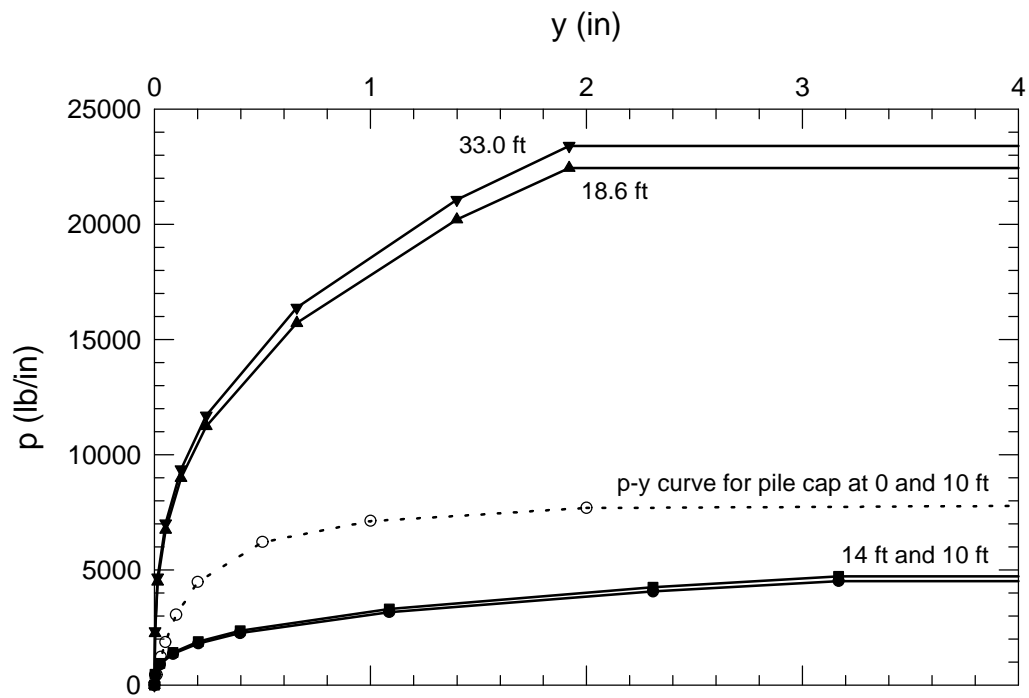
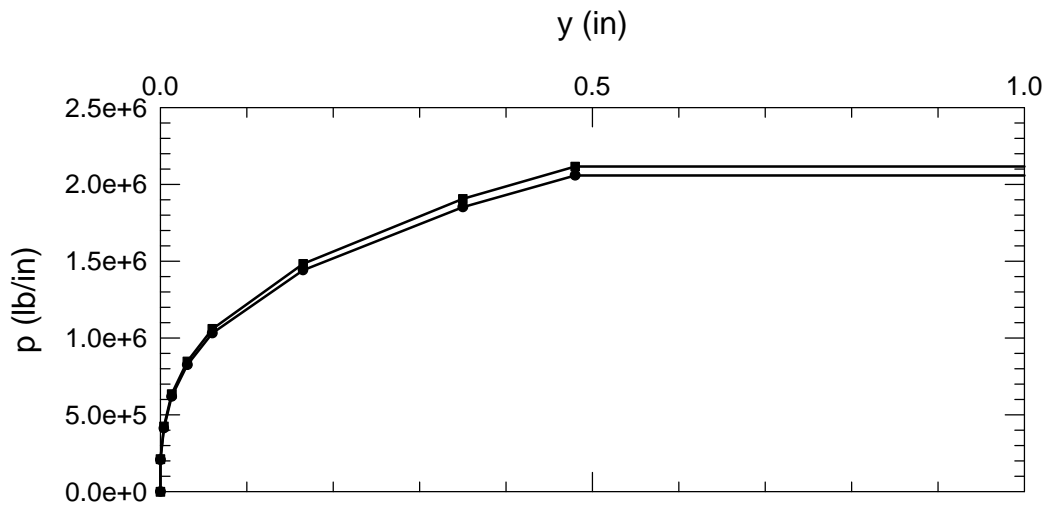


Figure 7.29. Comparison between calculated and measured responses of SE cap backfilled with New castle sand.



(a) p-y curves for stiff clay at 0, 10, 14, 18.6, and 33 feet below grade.



(b) p-y curves for caliche layer at 14.1 and 18.5 feet below grade.

Figure 7.30. "Group-equivalent pile" (GEP) p-y curves for the Zafir and Vanderpool (1998) case study.

Ultimate Capacity Calculation Sheet

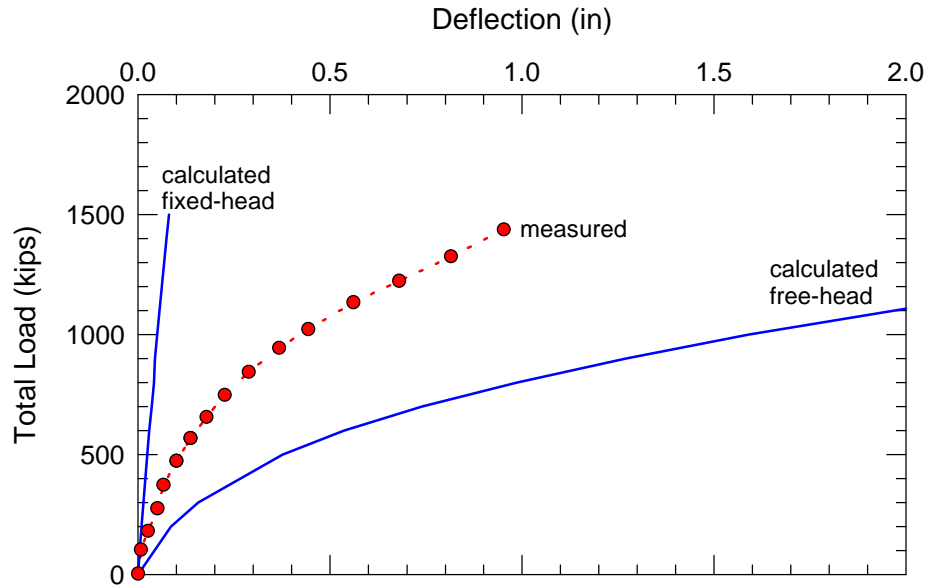
Created by R.L. Mokwa and J.M. Duncan - August 1999

Date: 9/1/99
 Description: Zafir and vanderpool case study
 Engineer: RLM

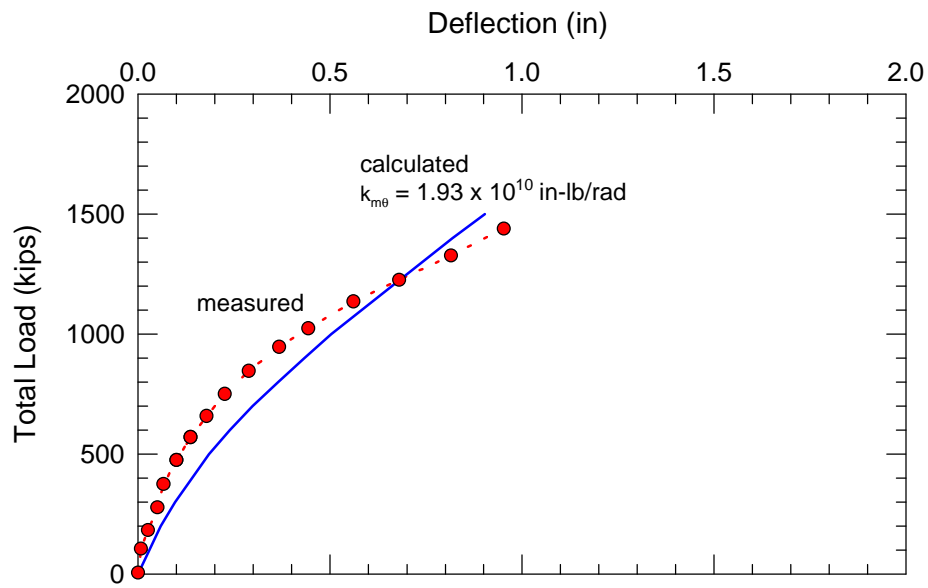
Input Values (red)

| | | |
|--|--------------------------------|---------------|
| cap width, | b (ft) = | 11.00 |
| cap height, | H (ft) = | 10.00 |
| embedment depth, | z (ft) = | 0.00 |
| surcharge, | q_s (psf) = | 0.0 |
| cohesion, | c (psf) = | 3000.0 |
| soil friction angle, | ϕ (deg.) = | 0.0 |
| wall friction, | δ (deg.) = | 0 |
| initial soil modulus, | E_i (kip/ft ²) = | 3000 |
| poisson's ratio, | ν = | 0.33 |
| soil unit weight, | γ_m (pcf) = | 125.0 |
| adhesion factor, | α = | 1.00 |
| Δ_{max}/H , (0.04 suggested, see notes) = | | 0.04 |
| <i>Calculated Values (blue)</i> | | |
| K_a (Rankine) = | | 1.00 |
| K_p (Rankine) = | | 1.00 |
| K_p (Coulomb) = | | 1.00 |
| $K_{p\phi}$ (Log Spiral, soil weight) = | Rankine Kp | |
| K_{pq} (Log Spiral, surcharge) = | Rankine Kp | |
| K_{pc} (Log Spiral, cohesion) = | Rankine Kp | |
| E_p (kip/ft) = | | 66.25 |
| Ovesen's 3-D factor, R = | | 1.00 |
| k_{max} , elastic stiffness (kip/in) = | | 6708.4 |
| phi = 0 Solution | | |
| P_{ult} (kips) = | | 1096.3 |

Figure 7.31. Summary worksheet from PYCAP for the Zafir and Vanderpool case study.



(a) Fixed-head and free-head boundary conditions.



(b) Rotationally restrained pile-head boundary condition.

Figure 7.32. Calculated responses for the Zafir and Vanderpool (1998) case study.

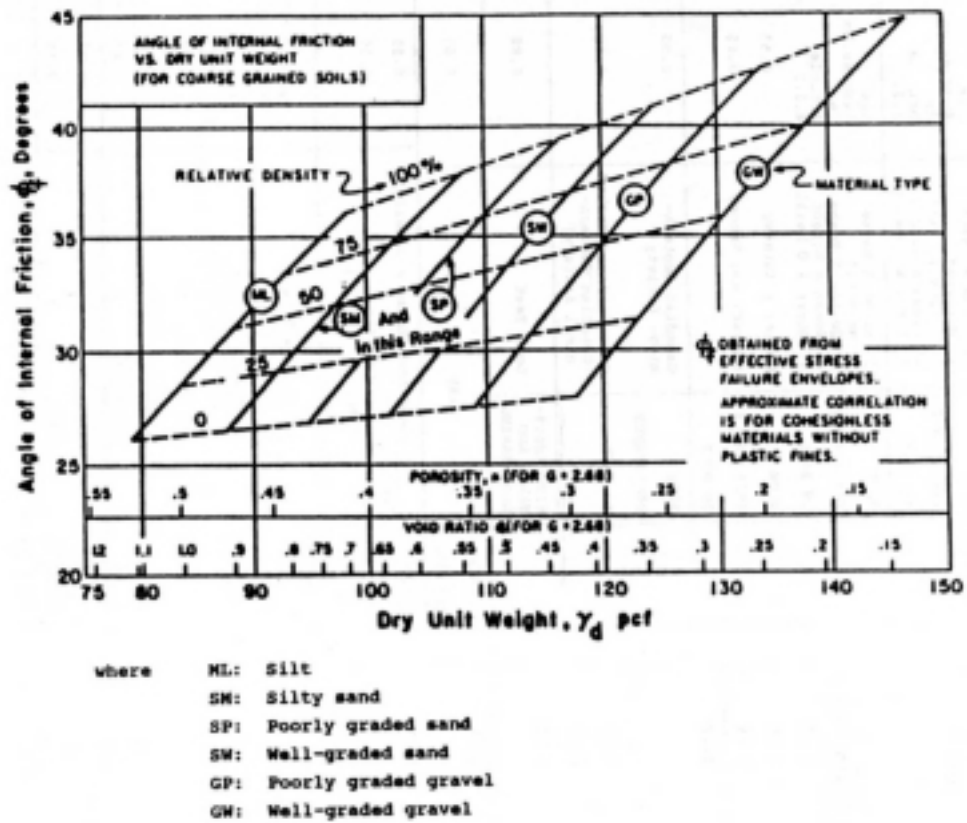


Figure 7.33. Approximate relationship between the friction angle and dry unit weight of granular soils. (After NAVFAC 1982)